

Stony Brook University



OFFICIAL COPY

The official electronic file of this thesis or dissertation is maintained by the University Libraries on behalf of The Graduate School at Stony Brook University.

© All Rights Reserved by Author.

Roles of Zinc and Iron on Bone Health in a Rat Model of Osteoporosis

A Thesis Presented

by

Danhua Yan

to

The Graduate School

in Partial Fulfillment of the

Requirements

for the Degree of

Master of Science

in

Materials Science and Engineering

Stony Brook University

May 2014

Stony Brook University

The Graduate School

Danhua Yan

We, the thesis committee for the above candidate for the
Master of Science degree, hereby recommend
acceptance of this thesis.

T.A. Venkatesh

Associate Professor

Department of Materials Science and Engineering

Yizhi Meng

Assistant Professor

Department of Materials Science and Engineering

Stefan Judex

Professor

Department of Biomedical Engineering

This thesis is accepted by the Graduate School

Charles Taber

Dean of the Graduate School

Abstract of the Thesis

Roles of Zinc and Iron on Bone Health in a Rat Model of Osteoporosis

by

Danhua Yan

Master of Science

in

Materials Science and Engineering

Stony Brook University

2014

Bone is one of the most vital organs in animals, serving as both structural and protective functions. Remodeling of bone is an important indicator of bone health, and disorders in bone remodeling may lead to bone diseases such as osteoporosis. Osteoporosis increases risk of bone fracture and even death, and much more preferable to be happened in postmenopausal women due to great changes in hormones. Micronutrients, such as Zinc (Zn) and Iron (Fe), would as well influence bone health in different manners. That Zn would promote bone health is widely accepted, for the reasons Zn increases osteoblast cell proliferation and differentiation, inhibits osteoclast cell activities, and forms alkaline phosphatase that does help to maintain bone metabolism. Diseases caused by Fe overload is usually related to osteoporosis. Ferric ion could facilitate osteoclast differentiation, inhibit osteoblast and alkaline phosphatase activities, and interfere with hydroxyapatite crystal growth and depositions. However, changes of concentrations and distributions for Zn and Fe in osteoporotic bones are seldom studied.

In this thesis, ovariectomized rat femur bones are used as a model of postmenopausal osteoporosis. Rats from different ages and health conditions are categorized as 6 AM (6-month age matched control), 6 OVX (6-month ovariectomized control), 12 AM (12-month age matched control), 12

OVX (12-month ovariectomized control). The trace elements Zn and Fe is studied through Synchrotron Radiation X-Ray Fluorescence (SRXRF). Elemental maps are used to observe changes in distribution, and further quantitative analysis is used to discover changes in concentration among different animal groups.

Both the decrease of Zn and the increase of Fe are significant from healthy to osteoporotic bones ($p < 0.05$). In the meanwhile, accumulation of Zn ($p < 0.05$) and Fe ($p > 0.1$) is also observed over age in healthy groups. Both elements show changes in distribution, that healthy animals present a more even distribution while in OVX groups the tendency of aggregation is observed. These results agree with most of the predictions and add evidence for effects of Zn and Fe on bone health. Hypothesis is further made to rationalize the changing trend observed and explain mechanisms behind.

Table of Contents

CHAPTER 1	INTRODUCTION.....	1
1.1	Bone Biology.....	1
1.1.1	Bone Structure	1
1.1.2	Bone Remodeling and Osteoporosis.....	3
1.2	Micronutrient.....	4
1.2.1	Micronutrients and Bone Health.....	4
1.2.2	Micronutrient Zinc (Zn).....	5
1.2.3	Micronutrient Iron (Fe).....	6
CHAPTER 2	HYPOTHESIS AND OBJECTIVE	8
CHAPTER 3	MATERIALS AND METHODS	9
3.1	Samples Preparation.....	9
3.2	Materials Characterization	10
3.2.1	Scanning Election Microscope (SEM).....	10
3.2.2	Energy-Dispersive X-Ray Spectrometer (EDX).....	10
3.2.3	Synchrotron Radiation X-Ray Fluorescence (SRXRF)	12
3.2.4	Further Images Processing: ImageJ	13
CHAPTER 4	RESULTS.....	14
4.1	Scanning Electron Microscope (SEM) Results	14
4.2	Energy-Dispersive X-Ray Spectrometer (EDX) results.....	17
4.3	Synchrotron Radiation X-Ray Fluorescence (SRXRF) Results.....	18

4.3.1	SRXRF maps for Ca	18
4.3.2	SRXRF maps for Fe.....	22
4.3.3	SRXRF maps for Zn	27
4.3.4	Quantification of elements.....	31
CHAPTER 5 DISCUSSION		34
5.1	Fe and osteoporosis	34
5.2	Zn and osteoporosis.....	36
CHAPTER 6 CONCLUSION AND FUTURE WORK.....		38
REFERENCES		39

List of Figures

Figure 1 Cross-section of bone and its cellular structure.....	2
Figure 2 General pattern of bone growth for postmenopausal women.....	3
Figure 3 (a) SRXRf instrument setup at NSLS X26A; (b) Schematic diagram of attenuation length; (c) Schematic diagram of SEM and EDX scan area; (d) Schematic diagram of SRXRf scan area.....	11
Figure 4 SEM images of 6 month AM group	14
Figure 5 SEM images of 6 month OVX group.....	15
Figure 6 SEM images of 12 month AM group	15
Figure 7 SEM images of 12 month OVX group.....	16
Figure 8 EDX results of 12 month OVX bone #82 (a) SEM image of region of interest (ROI); (b) Overlay of Ca, P EDX maps and SEM image of ROI; (c) Ca EDX map of ROI; (d) P EDX map of ROI.....	17
Figure 9 Comparison of SEM images, Optical Microscope images and SRXRf Ca maps for each tested bone sample	19
Figure 10 Ca maps in color scale.....	21
Figure 11 Overlay map of Fe (red) and Ca (blue) of sample #119 (6 OVX)	22
Figure 12 Fe maps in color scale	24
Figure 13 Fe/Ca ratio maps in color scale	25
Figure 14 Curve for distribution of Fe/Ca ratio in different groups (a) 6 AM; (b) 12 AM; (c) 6 OVX; (d) 12 OVX	26
Figure 15 Overlay map of Fe (red) and Ca (blue) of sample #119 (6 OVX)	27
Figure 16 Zn maps in color scale.....	28
Figure 17 Zn/Ca ratio maps in color scale.....	30
Figure 18 Curve for distribution of Zn/Ca ratio in different groups (a) 6 AM; (b) 12 AM; (c) 6 OVX; (d) 12 OVX	31

Figure 19 (a) SRXRF spectra of 12-month-age samples; and bar charts of average atomic molar concentration with standard deviation (error bar) of different elements (b) Ca; (c) Fe; (d) Zn ... 32

Figure 20 Briefly schematic diagram of new hypothesis of bone mineral 35

Figure 21 Zn/Ca atomic concentration ratio with standard deviation (error bar)..... 37

List of Tables

Table 1 Bone block samples group and testing information.....	9
Table 2 Comparison of porosity calculated by Micro-CT and SRXRF images	20

Acknowledgments

I would like to express my appreciation and thanks to my advisors, Dr. T.A. Venkatesh and Dr. Yizhi Meng, they have been tremendous mentors for me. I would like to thank them for encouraging me throughout the research and supporting me when I needed help. Also I would like to thank Dr. Stefan Judex for being one of my thesis readers and committee members, and for his suggestions and help during my research.

In addition, I would like to appreciate Sue Wirick and Antonio Lanzirotti, staff at NSLS X26A, for their kindness and guidance on my experiments. A special note for Sue, she is always happy to help me when I encounter difficulties about data processing, and also gives me valuable advices. I would also like to thank Fernando Camino, staff at CFN, for his time spending with me to optimize the SEM images and his advices on sample coating.

My senior fellow Derek Rammelkamp is friendly and helpful as well. Also a thank you to Kaushik Chava, for the reason that his previous work is a good foundation for my research, and his help at the very beginning when I was completely new to this project.

At last, I would thank all my friends who are supporting me during the tough days. Most importantly, thank my Dad and Mom for their endless love and support.

CHAPTER 1 INTRODUCTION

1.1 Bone Biology

Bone is one of the most vital parts throughout animals and human beings, serving as the function of providing body structure, protecting organs and assisting movement. Skeleton seems inert, however, bone is actually an active organ composed of cells and tissue in a continual state of living activity. Minerals and protein matrix together contribute to the bone formation, providing the unique property of bone, durable but lightweight and flexible. Around 65 % of bone is made from an inorganic mineral called hydroxyapatite, lies in the crosslinking protein matrix, with the chemical formula $\text{Ca}_{10}(\text{PO}_4)_6(\text{OH})_2$. Besides Calcium (Ca) and Phosphorus (P), other minerals such as Magnesium (Mg), Sodium (Na), Potassium (K) and citrate anions are also contained in bone, which are conjugated to hydroxyapatite instead of presenting their own crystals. The other 35 % of bone is an organ protein matrix, mostly of which is type I collagen, providing scaffolding for bone minerals to deposit on¹.

1.1.1 Bone Structure

There are two types of bone tissue primary based on their morphology. One is called cortical bone, also compact bone, and the other one is called trabecular bone, also spongy or cancellous bone (see *Figure 1*). Cortical bone refers to the outer surface of bone, accounts for about 80 % of the total skeleton. Though dense, cortical bone has micro openings for blood vessels and nerves to pass through. Trabecular bone accounts for the remaining 20 % skeleton, covered by cortical bone, located mainly in long bones, flat bones and spinal vertebrae. Cortical bone and trabecular bone share the same mineral composition and protein matrix components, and the difference lies in their microstructure and porosity. Trabecular tissue is much less dense and experiences remodeling and turnover much faster than cortical bone².

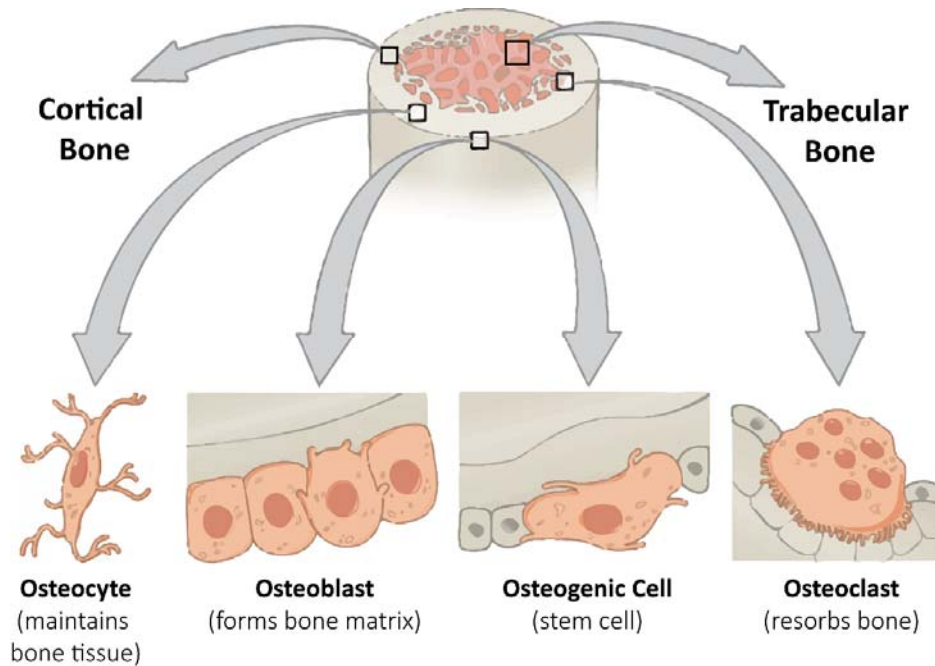


Figure 1 Cross-section of bone and its cellular structure (Edited by author based on image from Wikipedia³.)

At cellular magnitude, different types of bone cells can be observed (see *Figure 1*), such as osteoblasts, osteoclasts, osteocytes and so forth. Among these bone cells, Osteoblasts and osteoclasts are highly related to bone remodeling and turnover. Osteoblasts are cells that function in groups to form protein matrix which further mineralizes to become bone tissue. Osteoblasts have receptors for estrogen, Vitamin D and parathyroid hormone which thus become factors effecting bone health. An enzyme called alkaline phosphatase which is required in the mineralization process is also a product of osteoblasts. Osteocytes are the mature form of osteoblasts after mineralization. In contrast with osteoblasts, osteoclasts are bone cells that resorb bone tissue and release minerals. Osteoclasts contain enzymes and acids to break down protein matrix and insoluble minerals. Bone formation and resorption are always accompanied with each other, meanwhile osteoblasts and osteoclasts are together instrumental in controlling the amount of bone tissue and keep bone metabolism in balance³. Disorders in bone cells can result in different kinds of bone diseases.

1.1.2 Bone Remodeling and Osteoporosis

Human bone development will experience different stages. The size of bone grows quickly from birth through adolescence. Around age of 20 the bone will no longer gain its length but still accumulate bone mass gradually. Remodeling will take place after entering adulthood, and as people get older the rate of resorption will exceed formation. That is, inevitably, a process of losing in bone mass with aging (see *Figure 2*).

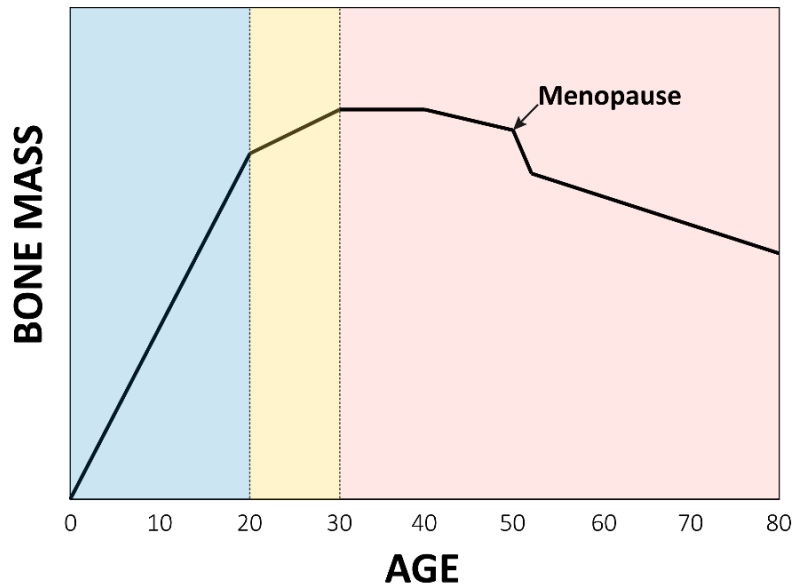


Figure 2 General pattern of bone growth for postmenopausal women (Illustrated by author based on the information and images from the reference²)

Balance of bone remodeling is important to bone health. Remodeling serves the function to maintain and repair bone tissue, adapt bone shape to new body weight, and control concentration of Ca in body fluids⁴. Trabecular bone has faster remodeling speed for its larger surface than cortical bone. When people grow older, rapid remodeling will cause fast bone loss as well. With this factor in mind, osteoporotic fracture will be more likely to happen in bones containing more trabecular tissue, such as hip and spine.

Bone can be characterized as osteoporosis when its bone mineral density drops 2.5 standard deviations below mean for young women according to WHO. Osteoporotic bone suffers great

possibility to fracture, and more seriously, leads to death. However, aging should not be the only one to be blamed for osteoporosis. In fact, roughly 67 % of osteoporosis patients over the age of 75 are female². That elder women are much more vulnerable to osteoporosis is due to the onset of menopause (see *Figure 2*). Deficiency in estrogen after menopause is followed by increasing of bone remodeling thus accelerating loss of bone⁵. Treatments of osteoporosis are usually aiming at providing patients with essential micronutrients to maintain bone health and hormones to reduce remodeling rate.

1.2 Micronutrient

Micronutrients, or so called trace elements are essential nutrients needed by human body only in a small quantities, including Zinc, Iron, and Copper and so forth. The suggested dietary intake of micronutrients are generally 100 mg/day⁶, which are in contrast with those macronutrients in amounts like proteins, fats and carbohydrates. However, these micronutrients play a significant and meaningful role in regulating the production of enzymes and hormones, helping human body to manage a range of different physiological activities, and also functions of the immune and reproductive systems⁷.

1.2.1 Micronutrients and Bone Health

As an active organ, the skeleton is comprised of living cells and tissue in a continual activity throughout the lifetime of human beings and different stages of bone biology. Thus micronutrients, such as Calcium (Ca), Vitamin D, Magnesium (Mg), Phosphorus (P), Zinc (Zn) and Iron (Fe), play a prominent role in metabolic processes of bone as well other human organs⁸.

Adequate micronutrients intake is known to have advantages in osteoporosis prevention and treatment⁹, among which Calcium (Ca) and Vitamin D are of greatest importance and have been widely studied⁹⁻¹⁰. Nowadays, it is clear that higher Ca intake is highly related to high bone mineral density comparing with lower intakes at various ages¹¹. In elder postmenopausal women, Ca intake around 400 mg/day shows significant reduction in bone loss rate than their age matched group¹². Vitamin D, together with Ca supplementation, also has convincing results in slowing down the

bone loss¹³. Inadequate intake of Ca and Vitamin D will have negative impact on calcium-regulating hormones, leading to Ca absorption reduction and higher possibility of fracture⁹. Magnesium (Mg) is also a major trace mineral in human body with both the structural and functional roles, especially crucial to human skeleton, for the fact that more than 50 % of the total amount of Mg can be found in bones. Mg co-localizes with hydroxyapatite of the bone, affecting the crystal size and strength of hydroxyapatite¹⁴. Low dietary intake of Mg might impair metabolism of minerals and bone mineralization, resulting in a risk factor of occurring osteoporosis¹⁵. Beside the micronutrients mentioned above, other trace elements like Phosphorus (P), Sodium (Na), Potassium (K), Fluoride (F) and so forth were proven to be essential in bone health⁹. Trace metals like Zinc (Zn), Iron (Fe) and Copper (Cu) play an important part in human body metabolism and also in bones. A supplementation combining Zn and Cu with Ca was able to reduce spinal bone loss in postmenopausal women¹⁶. However, effects of these elements on bones remain unclear compared with Ca or Vitamin D, and more studies are still needed to get better understanding. Recently, studies on roles of Zn and Fe on bones have revealed the importance of these trace metals in bone health.

1.2.2 Micronutrient Zinc (Zn)

Zinc (Zn) is an essential trace mineral in human body, which is present in normal foods naturally and available as a dietary supplement. Zn is involved in variety of cellular metabolism, and more than a hundred of enzymes require the catalytic function of Zn¹⁷. Moreover, Zn is involved in protein synthesis, DNA synthesis, protein synthesis and helping to maintain a healthy and effective immune systems¹⁸. Zn supports human body growth throughout newly born to adolescence¹⁹, also crucial for proper sense like smell and taste²⁰.

Human bones only contains around 0.0126 wt. % of Zn, but this accounts for 28 % total body Zn amount. Zn plays a structural role in bone, involving in the formation of the hydroxyapatite crystals²¹. Also, Zn is a key component to maintain bone metabolism, by means of promoting osteoblast cell proliferation and differentiation while inhibiting osteoclast cell activities *in vitro*²². Synthesis of osteoblast cells and cellular proteins requires Zn to activate aminoacyl-tRNA

synthetase. Moreover, Zn forms alkaline phosphatase and other hormones to promote bone mineralization²¹.

People should get enough Zn supplementation through daily diet for the reason that human body cannot store excessive Zn for further use²³, thus deficiency in Zn is a common health issue among poverty-stricken areas⁷. Zn deficiency can often show the symptoms of growth retardation and loss of appetite, also impaired immune function¹⁸. Retardation in bone growth is also a common finding in animals with Zn deficiency. Zn deficiency might lead to significant decrease in both cortical and trabecular bone mineral density and bone area. Also the Zn concentration in femur bone will decline along with Zn deficiency according to the experiments done in rats²¹. Disorders in bone metabolism will show up decrease in Zn vice versa. A study on human shows that Zn is lower in osteoporosis than normal bones²⁴.

1.2.3 Micronutrient Iron (Fe)

Similar to Zn, Iron (Fe) is also an important mineral for human beings, naturally present in foods and dietary supplements. Fe is usually known as an essential mineral to compose hemoglobin (an erythrocyte protein which transfers oxygen from the lungs to tissues) and to support myoglobin (a protein which provides oxygen to muscles)²⁵. What's more, Fe is required for growth, normal cellular functioning, and many other important cell processes such as synthesis of some hormones, connective tissue and DNA²⁶. Fe deficiency is the most common cause of anemia, where half of the 1.62 billion cases of anemia worldwide are due to Fe depletion²⁷.

Much of the excessive Fe can be stored in human body, contrast to Zn, in the form of ferritin or hemosiderin (a degradation product of ferritin) in bone marrow, liver and myoglobin for example. In the meanwhile, people tend to lose only a small amount Fe by means of urine and feces, or menstrual blood²⁵. Excessive Fe may be toxic, for its strong ability to generate free radicals and disability of human to regulate excretion of overload Fe²⁸. That means, overload of Fe may cause health issues to human body same as Fe deficiency. Fe overload is uncommon from dietary source, however, acute intake of more than 20 mg per kilogram body weight from medicines or

supplements can lead to symptoms like nausea, vomiting and faintness²⁹. Hemochromatosis, a disease caused by a mutation in the hemochromatosis gene, is also associated with Fe overload³⁰.

The role of Fe to bone health is somehow controversial. Fe is thought to be toxic to bone as osteoporosis is a common complication in diseases caused by Fe overload, for instance hereditary and thalassemia hemochromatosis. Experiments done on rats³¹ show significant changes in bones of rats with Fe-overloaded comparing with sham groups, including thinning of cortical bones and increasing of bone resorption and oxidative stress. The similar results were also observed in human according to a recently study³². In women group aged over 45 years old, higher serum ferritin concentration were associated with lower bone mineral density and greater risk to fracture. Possible mechanism of Fe toxicity has also been studied, showing that Fe overload in body will increase the reactive oxygen species index, which is used to characterize cellular metabolism which contributes to pathogenesis of osteoporosis. Additionally, suppression of alkaline phosphatase activity together with decline in the mineralized nodules is also observed, indicating an inhibiting function to osteoblast of Fe overload³³. However, on the other hand, some studies reported that dietary Fe supplement possibly has positive effect on bone health, for example spine bone in postmenopausal women⁸. One study based on bones of postmenopausal women find concentrations of Fe are lower in osteoporosis than in normal bones based on the method of high-resolution inductively coupled plasma mass spectrometry²⁴. Moreover, Fe restriction diet would increase porosity of trabecular bone as well³⁴. Thus, more study should be done to clarify the role of Fe in bones.

CHAPTER 2 HYPOTHESIS AND OBJECTIVE

Many researches have been done so far to clarify the pathologies of osteoporosis. However, there are still too many unknowns and mysteries left for us to explore. Micronutrients play an important role in bone metabolism. Besides widely studied components like Ca and Vitamin D, more and more studies about elements such as Zn and Fe are done for us to get better understanding about osteoporosis and other bone related diseases.

Zn will promotes activities of osteoblasts and inhibits osteoclasts, thus, Zn should be positively correlated with bone health. People have known that osteoporosis is usually accompanied with lower concentration of Zn in bone, and also Zn deficiency in human body would do harm to bone health vice versa. Nevertheless, morphologies and distribution of Zn other than concentrations are rarely studied.

Role of Fe is kind of double-edged sword. People need certain amount of Fe to maintain normal operation of human body, while excess Fe might be toxic to create health issues. It is already known to people that high Fe concentration in body and serum would result in decrease in bone mineral density. However, lower Fe concentrations were observed in osteoporotic bone than healthy bone in bone tissue alone. These interesting findings lead to confusions about role of Fe, hence deeper studies are also needed for a better understanding.

The overall objective of this thesis is to observe changes in distribution of Zn and Fe in rat femur bone with respect to age and disease state. With the help of Synchrotron Radiation X-Ray Fluorescence (SRXRF), maps of these trace elements can show different distributions for each group of animals. Based on literatures before, it is expected to see an overall decrease in Zn and increase in Fe concentrations in bones. Besides concentrations, it is assumed that changes in distribution such as aggregation might be possibly related to osteoporosis as well.

CHAPTER 3 MATERIALS AND METHODS

3.1 Samples Preparation

Ovariectomized (OVX) female Sprague – Dawley rats were proven to be a model for human osteoporosis³⁵, for their high bone turnover and subsequent bone loss is very much like human post-menopausal condition, and is widely regarded as a gold standard model for postmenopausal osteoporosis due to estrogen deficiency.

Femur bone samples of female Sprague – Dawley rats used in our characterization are obtained from research group of Dr. Stefan Judex, Department of Biomedical Engineering, Stony Brook University. All samples preparation procedures were under supervision of Institutional Animal Care and Use Committee of Stony Brook University. Each female Sprague – Dawley rat was individually raised in standard cages, allowed access to water and rodent chow freely, and weighed two times per week to monitor its body mass changes. Five-month-old adult female rats were divided into two mass-matched groups, ovariectomized control (OVX) and age matched control (AM). Rats from each control were sacrificed at age of 6 months and 12 months, and upon sacrifice, the left femoral diaphysis of each rat was taken and cleaned, then dehydrated in ethanol solutions at -20 °C. Samples were embedded in polymethyl methacrylate (PMMA) resin with proximal end exposed. Bone blocks were then cut longitudinal, with polish treatment on surface by abrasive silicon carbon papers and diamond suspension solution following.

Table 1 Bone block samples group and testing information (“X” means this sample has been tested by the method as noted.)

	6 Month							12 Month							
	AM			OVX				AM				OVX			
	230	114	33	119	121	116	117	36	82	70	71	86	40	41	42
SEM	X	X	X	X	X		X		X	X	X	X	X	X	
SRXRF	X	X		X	X				X		X	X	X		

Each individual rat was labeled as a unique number and these block samples were categorized to different groups as 6 AM (6-month age matched control), 6 OVX (6-month ovariectomized control), 12 AM (12-month age matched control), 12 OVX (12-month ovariectomized control) according to their age and bone health condition (see information indicated in *Table 1*)³⁶.

3.2 Materials Characterization

3.2.1 Scanning Electron Microscope (SEM)

The surface topography of the samples were imaged using a JEOL 7600F thermal field effect Scanning Electron Microscope (SEM) at Center for Functional Nanomaterials (CFN), Brookhaven National Laboratory (BNL), using 5 kV operation energy, 15 mm working distance and an LEI detector under low-magnification mode. These non-conductive PMMA block samples were coated with 20 nm thick carbon using a Gatan Model 681 High Resolution Ion Beam Coater to reduce charging in the atmosphere near the sample surface. Double sided carbon tape was further used to reduce chance of charging³⁷. Scans of different areas were combined to present an overall image of the bone surface (see *Figure 3c*).

3.2.2 Energy-Dispersive X-Ray Spectrometer (EDX)

JEOL 7600F SEM at CFN is also capable of possessing X-ray analysis instrumentation, namely, Energy-Dispersive X-Ray Spectrometer (EDX). The tests were operated using 10 kV energy, 8 mm working distance and an SEI detector under low-magnification mode. EDX map was used to clarify different phases and elements distribution, basically Calcium and Phosphorous. Test area of EDX was selected to contain both cortical and trabecular part of the bone (see *Figure 3c*).

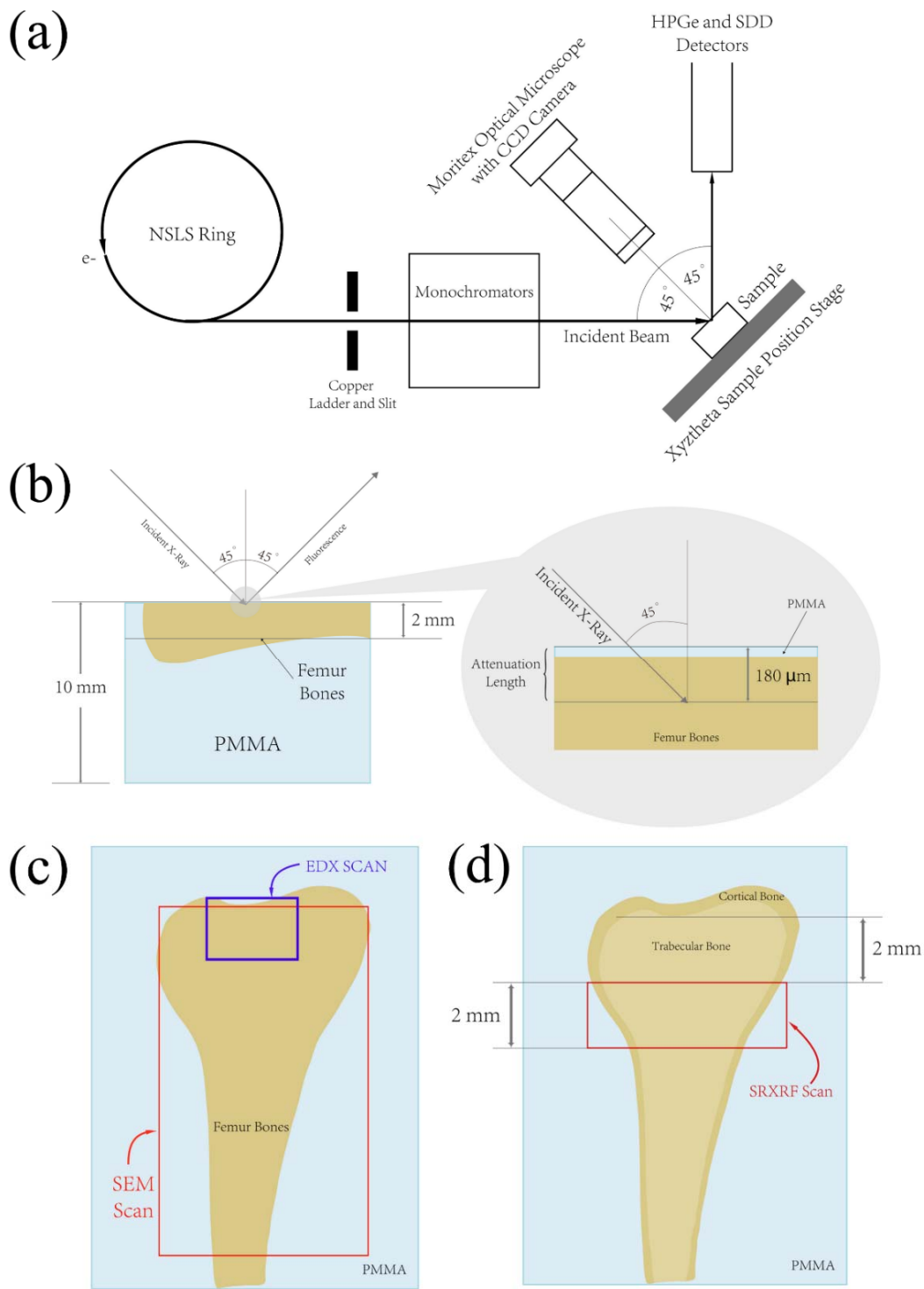


Figure 3 (a) SRXRF instrument setup at NSLS X26A (Based on information from X26A official website³⁸); (b) Schematic diagram of attenuation length; (c) Schematic diagram of SEM and EDX scan area; (d) Schematic diagram of SRXRF scan area.

3.2.3 Synchrotron Radiation X-Ray Fluorescence (SRXRF)

Synchrotron Radiation X-Ray Fluorescence (SRXRF) was conducted at Beamline X26A, National Synchrotron Light Source (NSLS), BNL. Synchrotron light has high energy and concentration X-ray, which is ideal for trace elements. Besides simple procedures and sample requirements, SRXRF can provide lower detection limits and higher sensitivities, and these advantages have been realized by an ever-growing scientific community³⁹.

The X-ray microprobe at beamline X26A is primarily operated in focused, monochromatic mode. Sample was mounted on the stage 45 ° toward the incident beam, while the energy-dispersive, 9-element Ge array detector resides at 90 ° toward the beam to eliminate the backgrounds from Compton scattering. An optical microscope was coupled to a digital camera for sample viewing (see *Figure 3a*)³⁸. Trace elements in femur bones, Zn and Fe, were studied by SRXRF using a mapping mode under 9-11 keV monochromatic beam of photons tuned by a Si (111) channel-cut monochromator, which is non-destructive to bones. Energy dispersive spectra and elemental maps were collected using a dwell time of 0.1 s/pixel and a step size of 0.01 mm to provide oversampling. The estimated attenuation length of the samples is about 180 μm, defined as the depth into the materials where the number of photons has decreased by 37 % (1/e) from the number of incident photons, which indicates that the photons cannot penetrate the bone and all the signals should come from the sample itself (see *Figure 3b*). The test areas were decided by comparing all the SEM images of the bones to ensure to include accurate and unique information for each group of animals. The top of each test area was 2 mm away from the bone growth plate, and test area was 2 mm wide, and a length long enough to cover all the bone tissue (see *Figure 3d*).

The fluorescence spectrum for each pixel was collected and then combined to generate SRXRF maps for different elements using software provided by X26A called XMap-Plotter³⁸. The math between different maps were also done by this software to create ratio maps.

NIST thin-film standard reference materials SRM 1832 and SRM 1833 were used for data quantification. Area concentration for each element was calculated by normalizing fluorescence peak intensity (counts) to SRM 1832 and SRM 1833 and converting to weight concentration per

area ($\mu\text{g}/\text{mm}^2$). Then these concentrations were converted to molar concentration for calculation of means and standard deviations of each group. Student's T-Test was performed to measure significant differences between mean values of related groups, while p -value smaller than 0.05 was recognized as highly-significant.

3.2.4 Further Images Processing: ImageJ

The porosity of the bone and the histogram of the element ratios were calculated by the ImageJ software. The basic concept of ImageJ is to count different pixels to achieve different analytical task. Generally, maps obtained from the SRXRF were analyzed after adjusting the brightness and contrast as suggestion by the software. Then the image was converted into an 8-bit map for threshold adjust or histogram analysis later on. Threshold process for trabecular porosity analysis, which is done by the software automatically, will turn the picture into the color mode of either black or white, which will be easy for computer to recognize the holes and calculate the porosity. Histogram of element ratio was based on the of digital value expression for color greyscale of each pixel in computer (256 level of darkness intensities from white to black for 8-bit images, expressed as numbers from 0 to 255). Each color intensity represents a range of ratio, thus different pixels with different greyscale will be categorized into different ratio range, and the distribution of ratios then can be easily obtained. Integral area of histogram was normalized to 1 to eliminate the inaccuracy of relative intensities caused by different image size. All the image processing tasks were done by computer and no subjective manual adjustments were made to ensure the reliability of these results.

CHAPTER 4 RESULTS

4.1 Scanning Electron Microscope (SEM) Results

Bone block samples are tested by SEM to see the differences in surface morphologies between rat femur bones from different groups as 6 AM, 6 OVX, 12 AM and 12OVX. Three samples of each group adding up to twelve samples were tested to ensure horizontal and vertical comparison among each group. The overall picture of each bone sample was matching from images of different areas with an x25 magnitude.

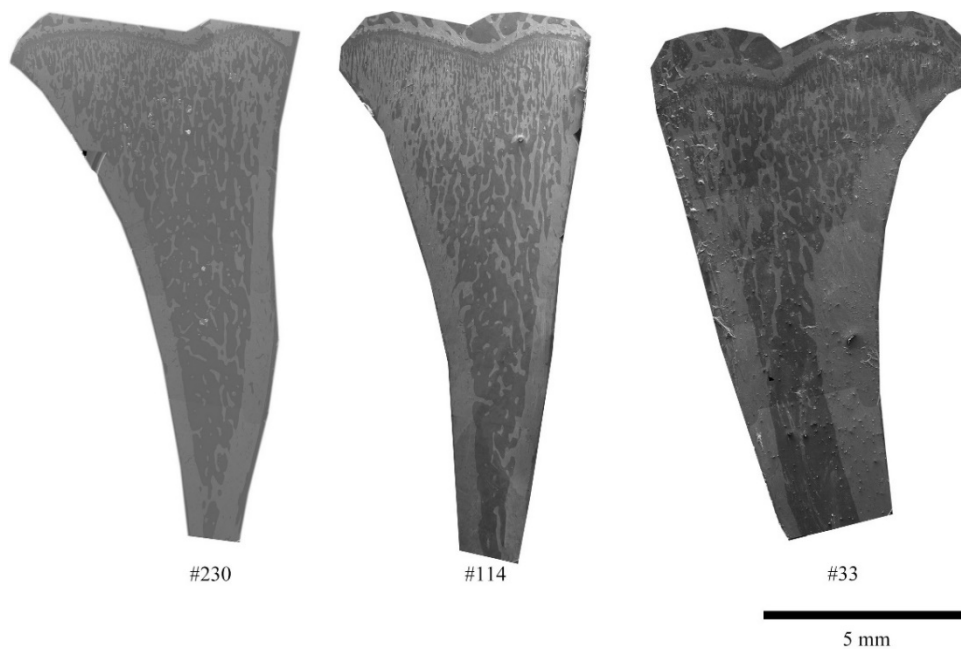


Figure 4 SEM images of 6 month AM group

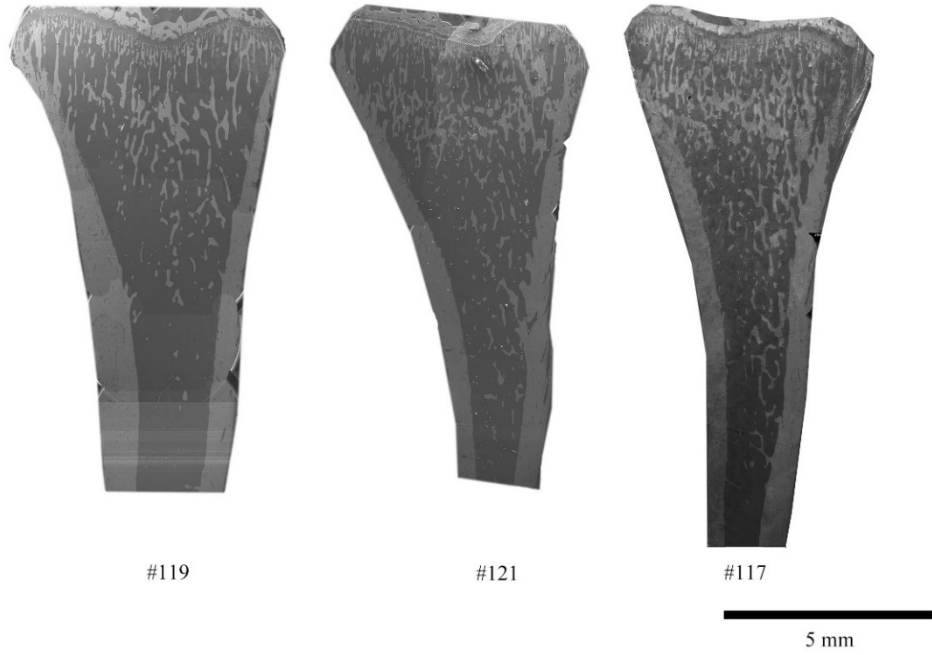


Figure 5 SEM images of 6 month OVX group

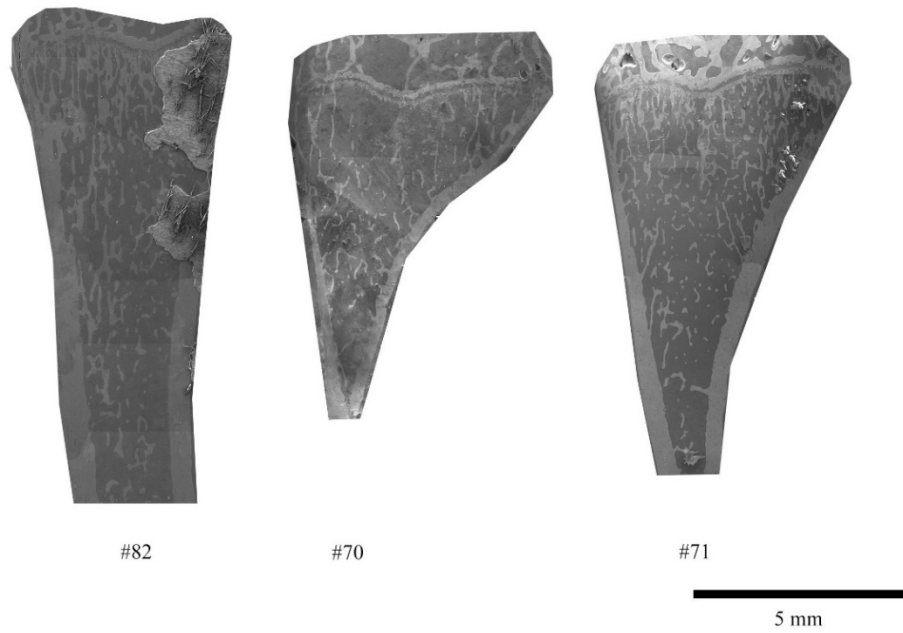


Figure 6 SEM images of 12 month AM group

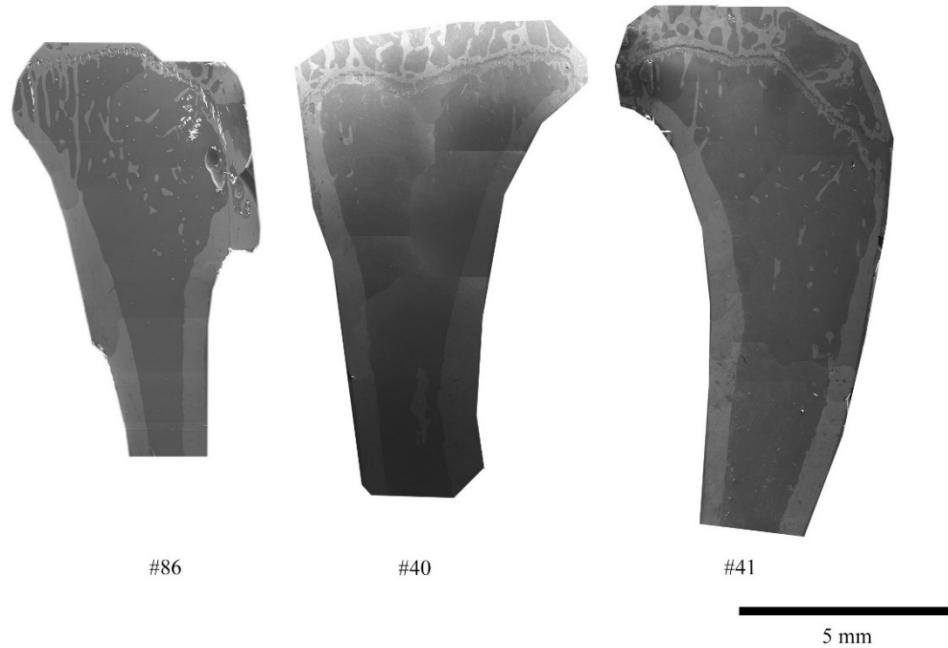


Figure 7 SEM images of 12 month OVX group

The cortical and trabecular part of the bone can be easily identified from four figures above (*Figure 4, Figure 5, Figure 6 and Figure 7*). The outer dense layer is the cortical bone while the inner porous part is the trabecular bone. All of these bone samples appear lighter phase and darker phase, and it is estimated that the lighter phase corresponds to minerals of the bone tissue according to its morphologies. This assumption is also confirmed in the EDX results later (see *Figure 8*). Although different individuals show up different shape of left femur bone and thickness of cortical bone, animals in the same group share similar features in trabecular bone. The trabecular bone gradually reduces from the growth plate to proximal end for all animals, and also decreases with aging. In the meanwhile, the amount of spongy bone starts to decline even one month after ovariectomizing (6 month OVX). After ovariectomizing for seven months (12 month OVX), the trabecular bone loses almost all its structure and the porosity of the trabecular bone goes up significantly. This trend is reasonable as osteoporosis will definitely reduce bone mineral density and deteriorate the bone microarchitecture.

4.2 Energy-Dispersive X-Ray Spectrometer (EDX) results

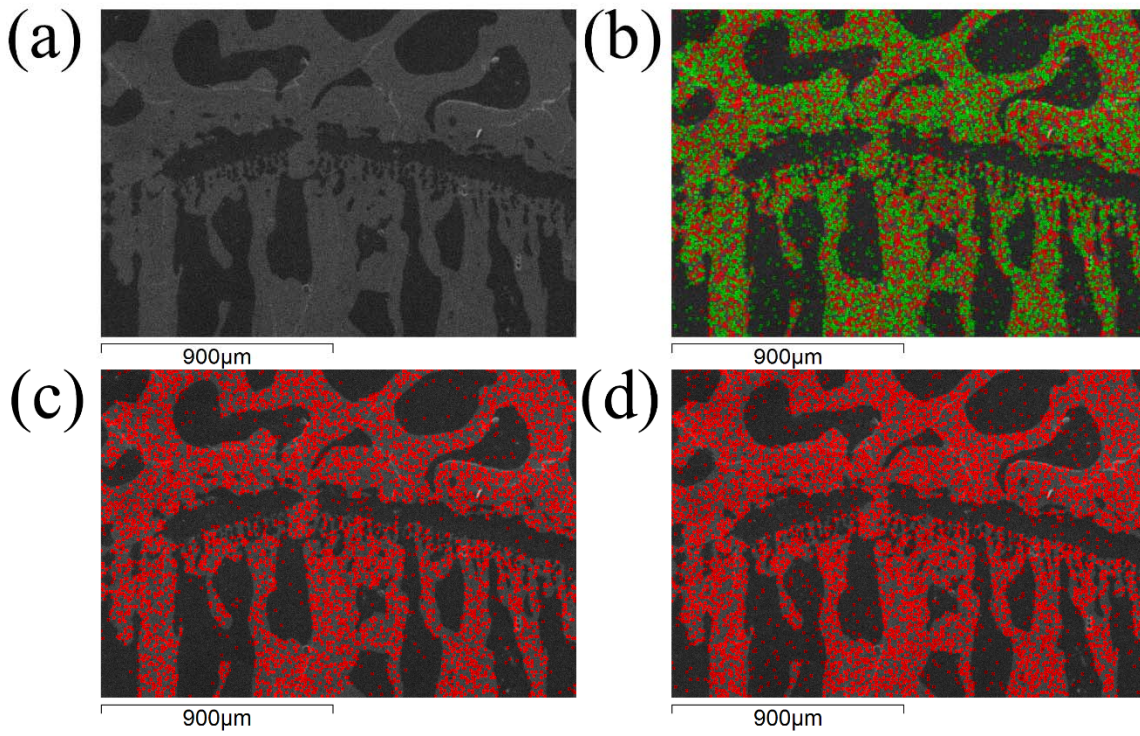


Figure 8 EDX results of 12 month OVX bone #82 (a) SEM image of region of interest (ROI); (b) Overlay of Ca, P EDX maps and SEM image of ROI; (c) Ca EDX map of ROI; (d) P EDX map of ROI.

EDX was done with SEM to clarify the component of different phases show up in SEM results. As stated above, the lighter phase of the SEM image is the mineral phase of the bone tissue. This statement is primarily based on the EDX maps showed in *Figure 8*. Calcium and Phosphorous are two key components of hydroxyapatite, which composes the mineral phase of bone. Both Ca element map and P element map are highly correlated with the lighter phase in this bone sample. Same results were obtained on different animals from previous work done by other student³⁷. The trend of changes in trabecular bone together confirm the certainty of the statement above.

The darker phase, however, cannot be defined for sure with EDX results. It can be estimated by knowledge that the darker part would be proteins in between minerals. The EDX of darker phase

(not shown) is basically made up with Carbon and Oxygen, which are distributed all over the sample no matter dark or light, indicating the possibility of being the PMMA resin itself alone.

The resolution of the EDX we used is unable to detect trace amount of elements, thus neither Zn nor Fe was observed from the EDX results. In this case, further SRXRF is required to see the distribution of Zn and Fe in bone tissue.

4.3 Synchrotron Radiation X-Ray Fluorescence (SRXRF) Results

The fluorescence spectra contain the full information of the bones. In this thesis, only Ca, Zn and Fe were extracted from the spectra for detailed study.

4.3.1 SRXRF maps for Ca

The elements of minerals in bones are primary Ca and P. Within the testing energy, Ca generated very strong signal but not for P. To our knowledge, Ca contents in bones can be regarded as constancy comparing to other trace elements, and thus been selected as a reference element to be normalized on. Also, there are plenty of studies on minerals in bones and hence Ca can be used to compare SRXRF with other experimental methods as well.

As stated above, the test areas were chosen based on the SEM images obtained to contain unique information for each animals. Then the Ca map for each animal was compared with the SEM results as they both present the morphology of Ca in bones. Images from optical microscope were also included for comparison (see *Figure 9*).

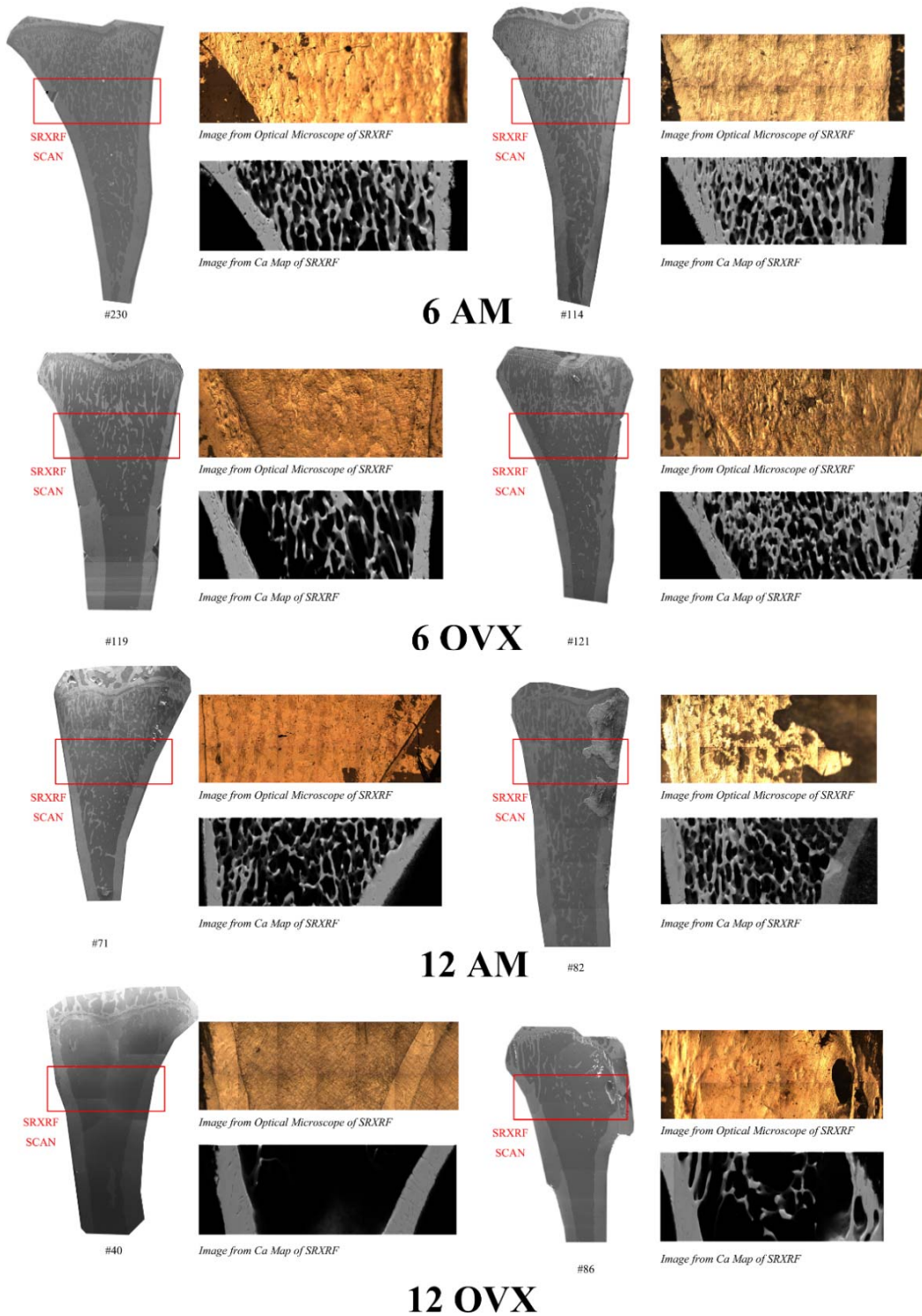


Figure 9 Comparison of SEM images, Optical Microscope images and SRXRF Ca maps for each tested bone sample

It can be easily identified that the SRXRF Ca maps present almost the same trabeculae structure as SEM images. Under optical microscope, the trabecular bone shows an uneven and rough surface while PMMA shows a relatively even and polished surface, which is agreed with both SRXRF and SEM results as well.

The porosity, defined as one minus volume of trabeculae over total bone volume ($1 - BV/TV$), was also calculated by ImageJ software (see *Table 2*). The porosity indicates a sharp drop of trabecular bone density in ovariectomized rats after 7 month of surgery (12 OVX). The porosity will go up with aging process as well, either in AM groups or OVX groups. However, the porosities of 6 month OVX rats are not significantly different ($p>0.2$) comparing with 6 month AM counterparts. Reasonable explanation of this phenomenon is that only 1 month after ovariectomizing wasn't long enough to observe symptoms of osteoporosis, since these rats from 6 OVX group were ovariectomized at age of 5 month. After body hormones changes and bone remodeling in the next 6 month, the symptoms became pretty obvious to be noticed in 12 OVX group.

Table 2 Comparison of porosity calculated by Micro-CT and SRXRF images

BV/TV	6 AM	6 OVX	12 AM	12 OVX
Micro-CT	N/A	N/A	0.24	0.03
SRXRF	0.38	0.21	0.31	0.09
	0.49	0.40	0.23	0.05

Comparing with Micro-CT results on Ca (see *Table 2*) in previous study done by other students⁴⁰, these results are not significantly different in statistics ($p>0.2$). The Micro-CT results were based on cross sections while SRXRF results were based on longitudinal sections, thus may raise a slightly differences between these two results due to the space distribution of trabecular bone. Together with comparison of SEM images and Optical Microscope images, it is rational to say SRXRF is reliable method to study bone elements based on maps for Ca.

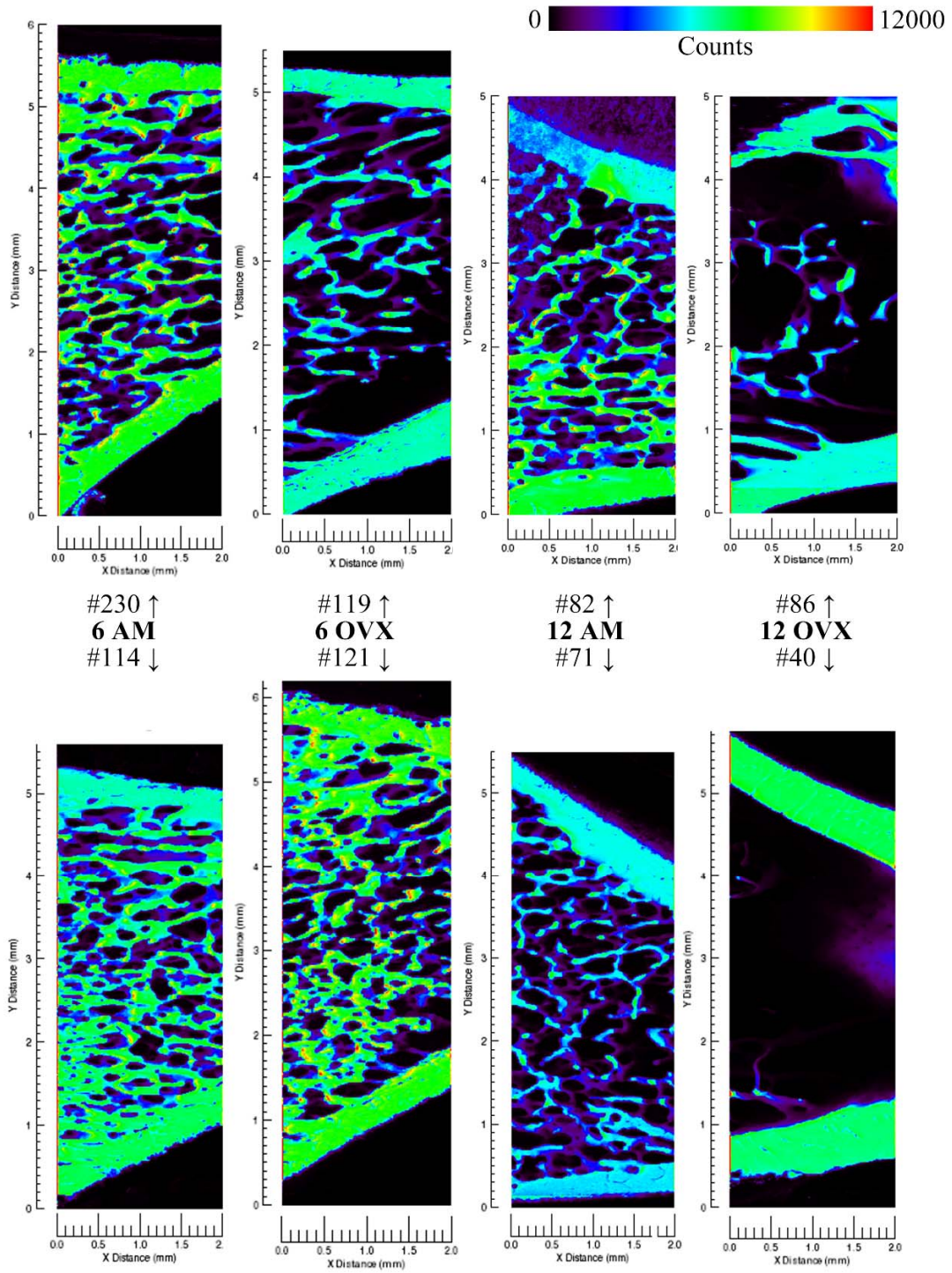


Figure 10 Ca maps in color scale

Ca map for each animal tested was put in the same color scale (0 – 12,000 counts, black for minimum and red for maximum) side-by-side (see *Figure 10*). Changes in trabeculae can be referred to measurement of porosity. Besides dramatically decline in trabeculae of 12 OVX group, trends or differences in Ca concentration can hardly tell in neither cortical nor trabecular bone from rest of these samples. Although these maps are 2-Dimensional, a 3-Dimensional structure can be observed due to a depth that X-ray beam can penetrate. As the thickness of PMMA over the bone surface cannot be measured accurately, the exact depth of sample signals cannot be normalized when comparing between different samples. Same issue also exists in Zn and Fe maps, however the penetration depth of X-ray for the same sample is fixed, and then Ca maps were used to normalize the Zn and Fe concentration of different samples. This will be discussed further in the later section.

4.3.2 SRXRF maps for Fe

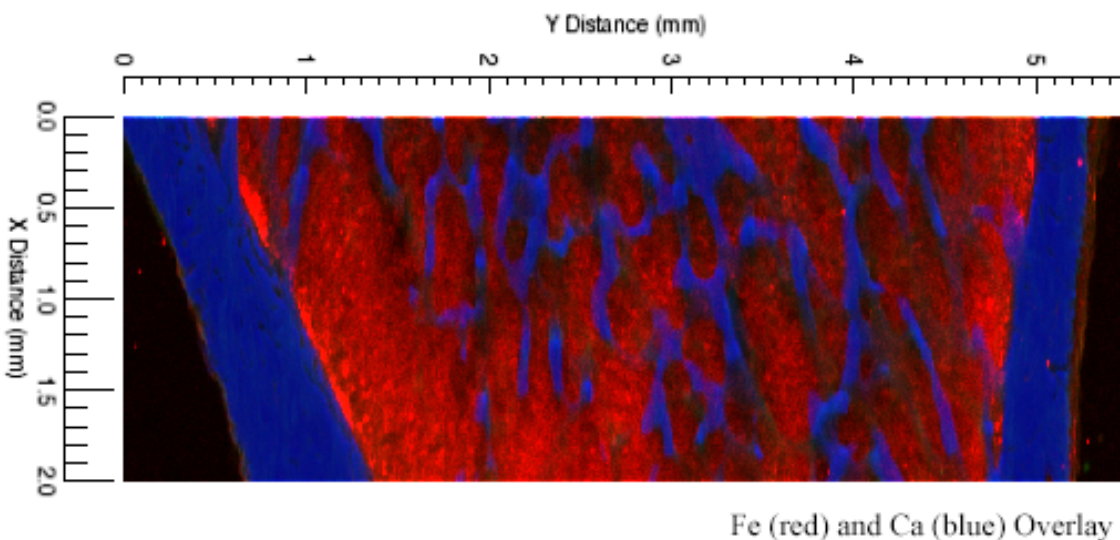


Figure 11 Overlay map of Fe (red) and Ca (blue) of sample #119 (6 OVX)

In the beginning, it is necessary to have an idea about where Fe exhibits in the bone. *Figure 11* shows an example (#119, 6 OVX) of overlay map of Fe and Ca. The intensity for each element was adjusted to clearly show the overlay feature of these elements. Basically, Fe resides around trabeculae and is not included in the minerals both in cortical and trabecular bone. Some small

areas look like overlay (purple) around some trabeculae are most probably elements in different planar. Other samples (not shown) were also checked to ensure this phenomenon.

Fe map for each animal tested was put in the same color scale (0 – 625 counts, black for minimum and red for maximum) side-by-side (see *Figure 12*). Sample #230 has an overall high Fe concentration than any other sample tested. As sample #230 has a relatively same amount of Ca as sample #121 (see *Figure 10*), this high amount content of Fe may not be raised due to a thicker penetration of this sample. The reason for such high concentration is unknown, or may be explained as a special case for this individual. Test for more samples will help to clarify whether this sample is abnormal than others in the same group. Except sample #230, samples from OVX groups seem to have a slightly higher Fe concentration than relevant AM groups. Besides the absolute concentration of Fe, the distribution of Fe also changes with either aging or disease. Fe of AM groups has a relatively even distribution among trabeculae, and OVX groups tend to have clusters and aggregations in between trabecular bone.

To better compare Fe distribution of different samples and eliminate the error caused by different sample thickness, a Fe/Ca ratio map was generated to normalize Fe content to Ca as indicated above (see *Figure 13*). The amount of Ca can be regarded as constant as the counts of Ca is three orders of magnitude larger than Fe. Most parts of bone minerals are almost black in Fe/Ca ratio maps, for the reason that Fe isn't overlaid with Ca. Moreover, Ca signals from different depth plane will also decrease the value of Fe/Ca ratio. Thus, the significant increase in Fe/Ca ratio of sample #40 is not necessarily related to an increase in Fe contents, as a possible reason cannot be ruled out that the increase may be resulted from absence of Ca. However, it can be observed that in AM groups Fe has an average distribution while in OVX groups Fe tends to accumulate in larger pores of trabecular bone, which are usually resided at the edge of cortical and trabecular bone.

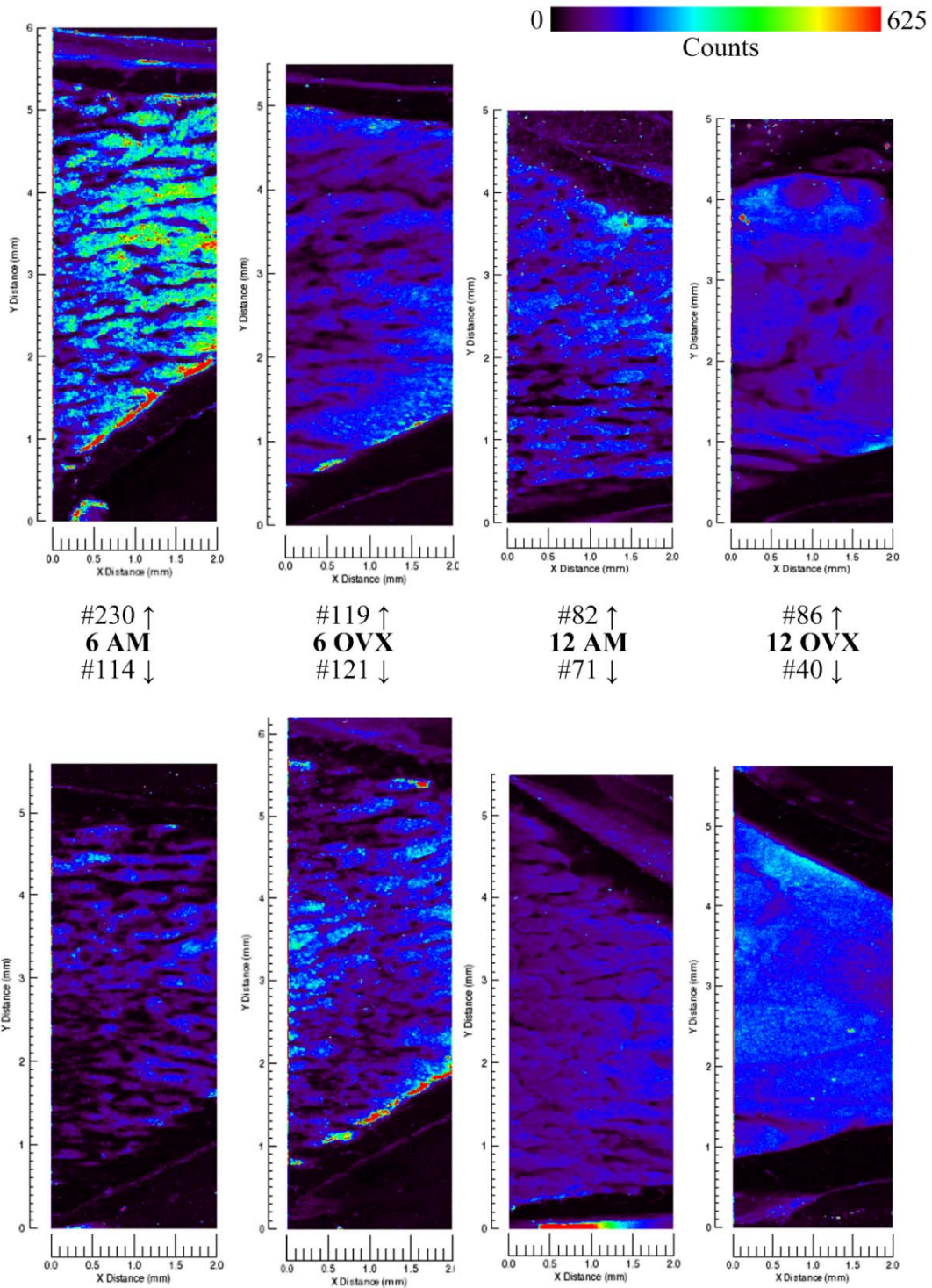


Figure 12 Fe maps in color scale

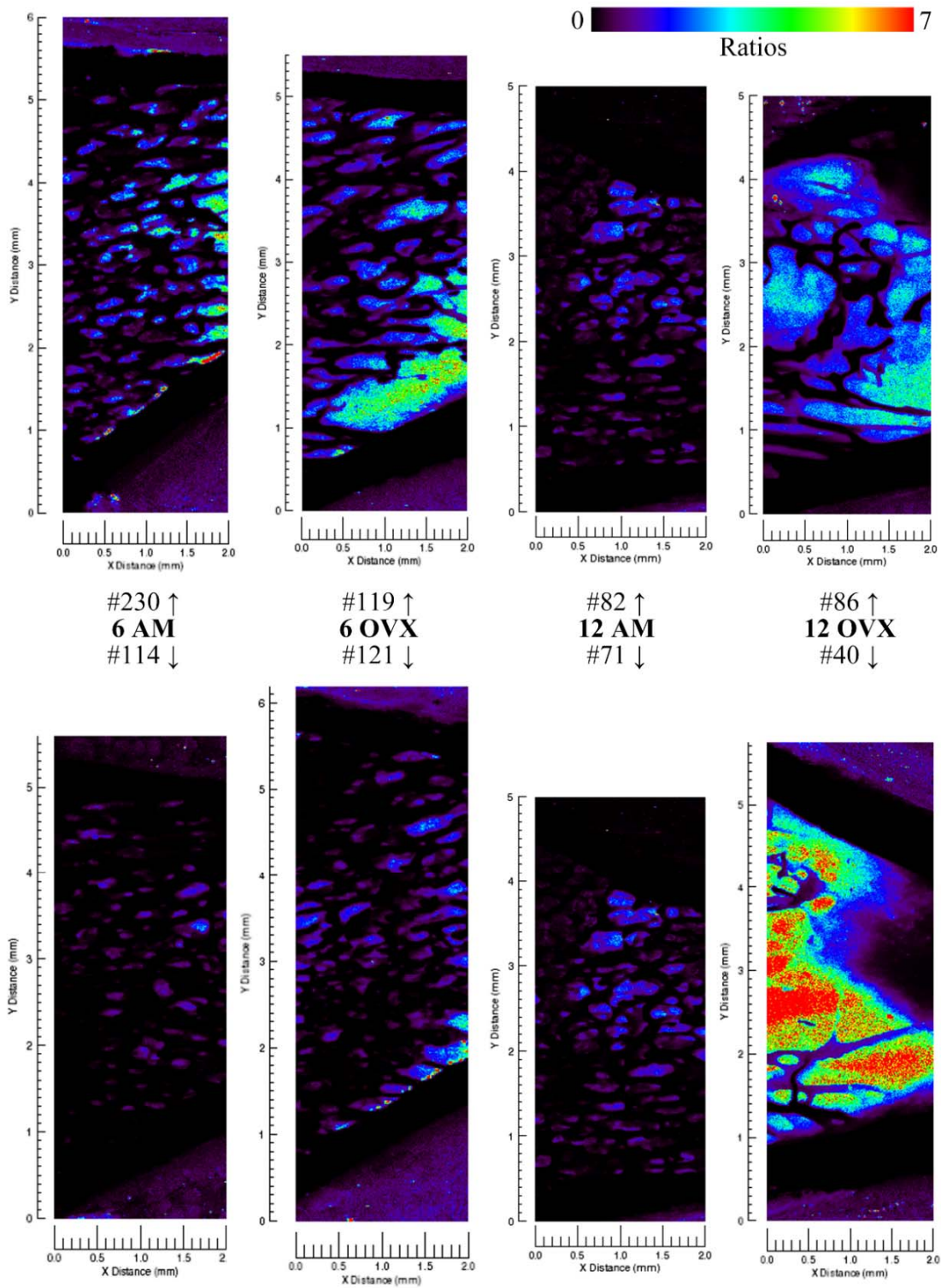


Figure 13 Fe/Ca ratio maps in color scale

The change in distribution of Fe/Ca ratio in trabeculae can also be reflected by the histogram curve of different samples (see *Figure 14*).

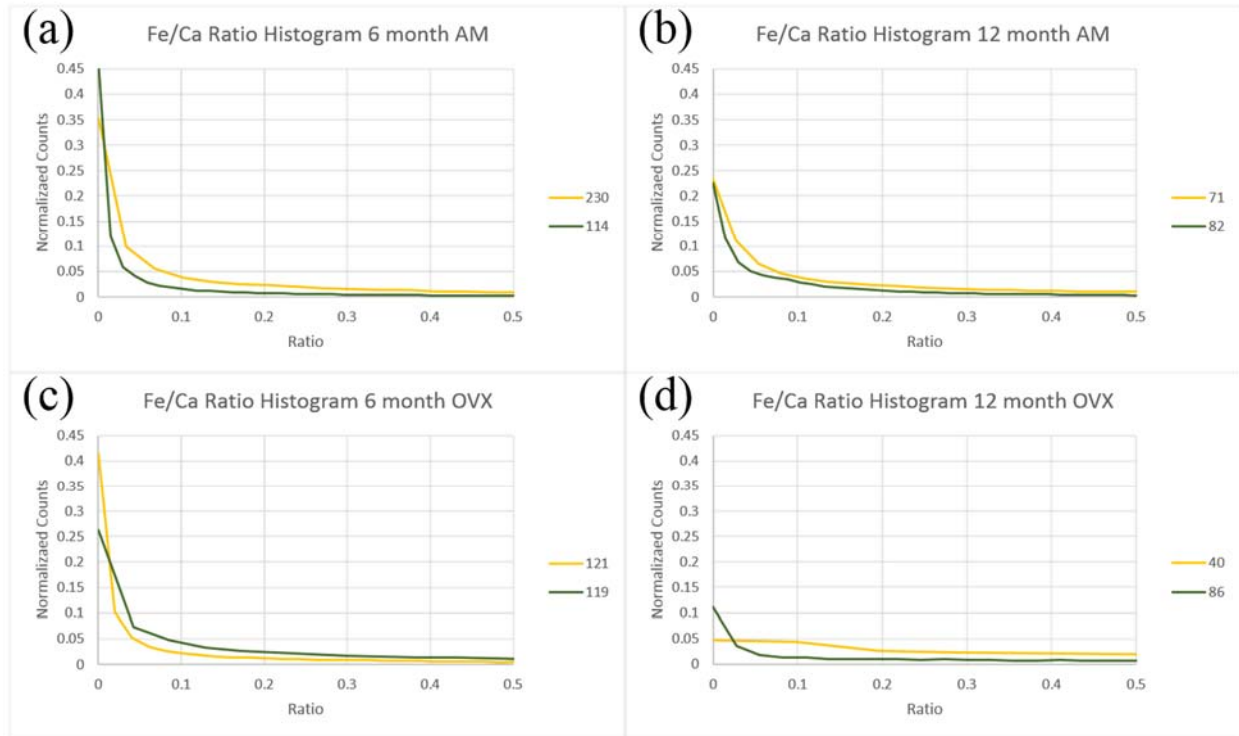


Figure 14 Curve for distribution of Fe/Ca ratio in different groups (a) 6 AM; (b) 12 AM; (c) 6 OVX; (d) 12 OVX

Samples from same group basically share the same distribution, and the peaks are broaden as ages go up. Decrease in peak intensities can be easily observed from young to old, healthy to ill, which is due to the decline of bone minerals (Ca). As all curves normalized to 1, the sharp decline in peak intensities would together lead to a broader peak. 6 AM group, 6 OVX group, 12 AM group and 12 OVX group has an average skewness of 13.77, 13.50, 10.12 and 6.52 respectively. The skewness may be an indicator of peak shift, suggesting a buildup in Fe with process of aging or disease.

4.3.3 SRXRF maps for Zn

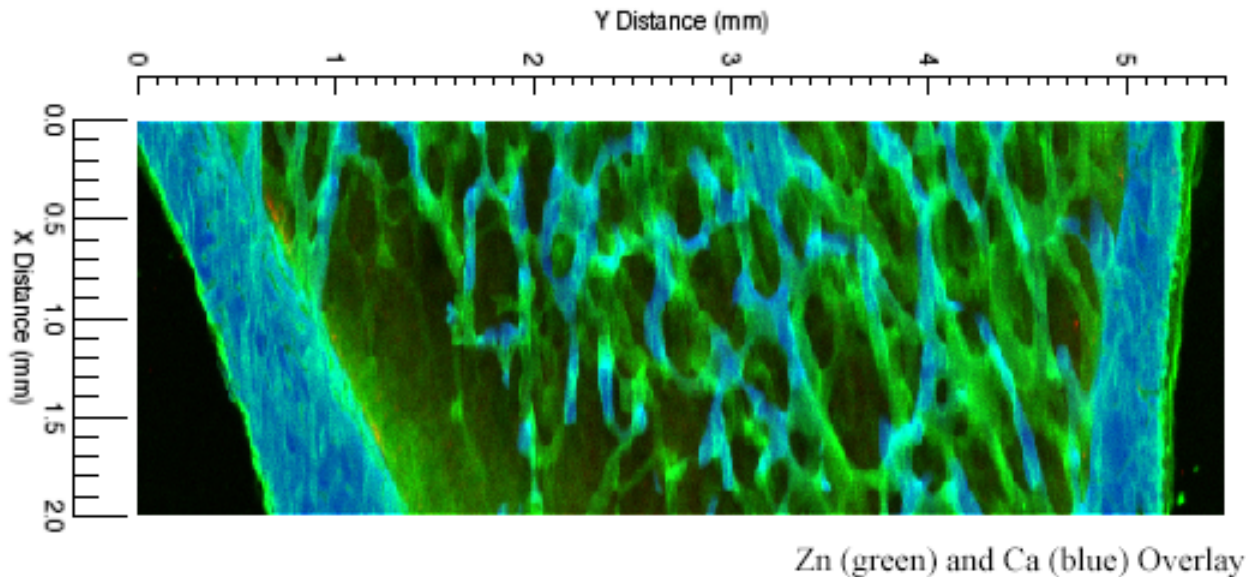


Figure 15 Overlay map of Fe (red) and Ca (blue) of sample #119 (6 OVX)

Figure 15 shows an example (#119, 6 OVX) of overlay map of Zn and Ca. The intensity for each element was adjusted to clearly show the overlay feature of these elements. Zn is a relatively abundant element in bone, widely distributed all over in cortical bone, trabecular bone and also bone matrix. Zn presents a cross-linking net structure, and part of the net is highly correlated with Ca structure. This can be well explained by previous understanding of formation of trabecular bone: Zn is contained in hydroxyapatite as minerals; while the structural framework termed as organic bone matrix is mainly comprised of proteins that require large amount of Zn. The minerals like Ca are deposited in this network to together form trabeculae⁴¹. Other samples (not shown) were also checked to ensure this observation.

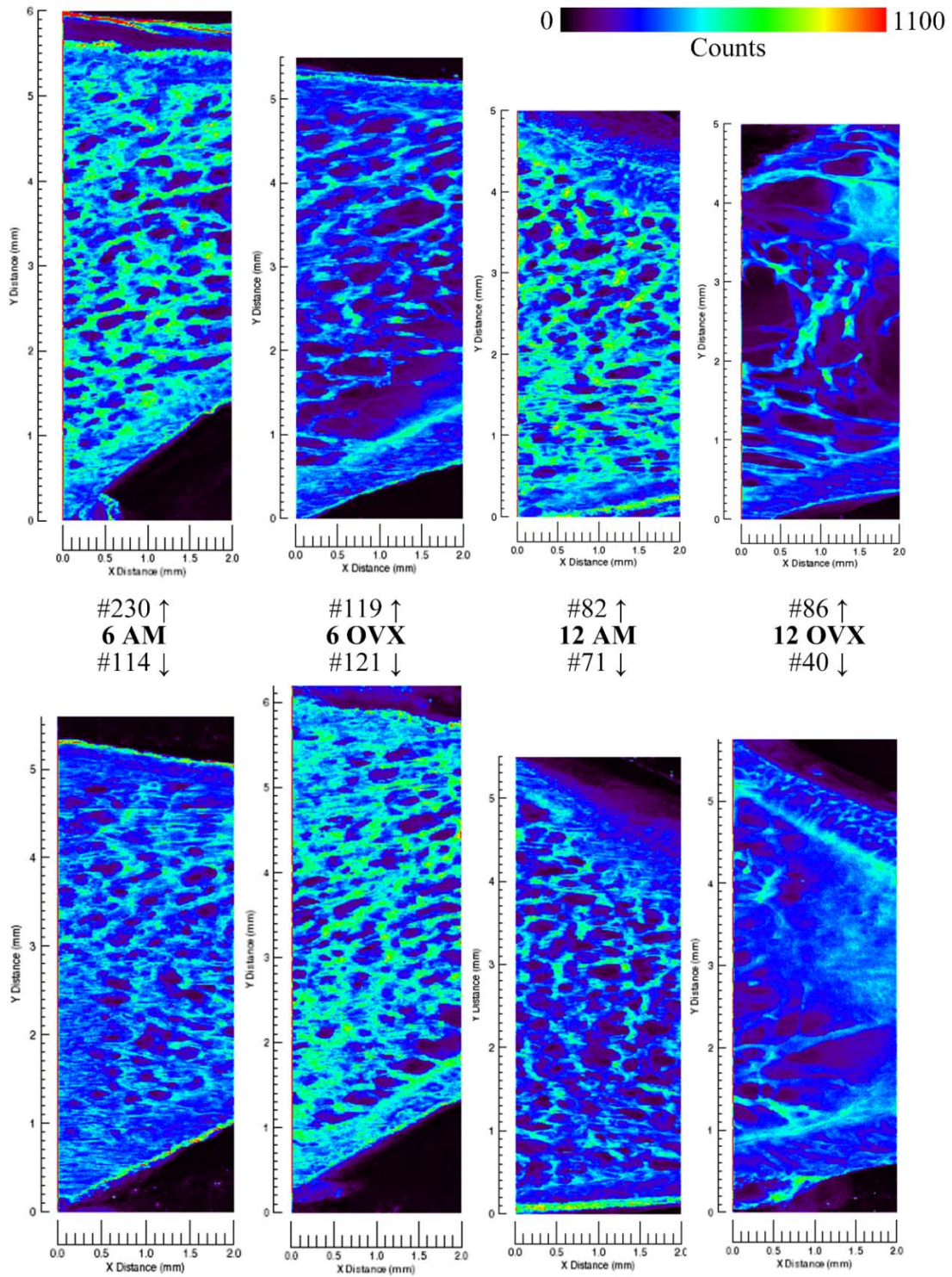


Figure 16 Zn maps in color scale

Zn map for each animal tested was put in the same color scale (0 – 1,100 counts, black for minimum and red for maximum) side-by-side (see *Figure 16*). The Zn amount in cortical bone seems don't change with age or disease, except a relatively higher counts in sample #121 and #230, which can be explained as a deeper X-ray penetration depth. In trabecular, each sample presents a darker framework structure and a higher trabeculae structure among these frameworks. When observe trabecular area of Zn map and Ca map for sample #40 carefully, Zn map shows a detailed cross-linking structure while Ca map has almost nothing left. This adds evidence for statement above, and indicates the decline in trabeculae with aging and disease can occur both in protein matrix structure and in minerals. It can also be observed that Zn tends to aggregate at the edge of cortical and trabecular bone in OVX groups.

To better compare Zn distribution of different samples and eliminate the error caused by different sample thickness, a Zn/Ca ratio map was generated to normalize Zn content to Ca as indicated above (see *Figure 17*). The amount of Ca can be regarded as constant as the counts of Ca is three orders of magnitude larger than Zn. The black part in the ratio maps is where minerals present, where the color part corresponds to remaining Zn in protein matrix. The significant increase in Zn/Ca ratio of sample #40 is not necessarily related to an increase in Zn contents, as a possible reason cannot be ruled out that the increase may be resulted from absence of Ca. However, it can be observed that in AM groups Zn has an average distribution while in OVX groups Zn tends to aggregate in place where protein frameworks and minerals are absent.

The change in distribution of Zn/Ca ratio in trabeculae can also be reflected by the histogram curve of different samples (see *Figure 18*). Samples from same group basically share the same distribution, and the peaks are slightly broaden as ages go up. Decrease in peak intensities and increase in peak width can be easily observed from young to old, healthy to ill. 6 AM group, 6 OVX group, 12 AM group and 12 OVX group has an average skewness of 7.36, 6.65, 5.76 and 3.15 respectively. The skewness may be an indicator of peak shift, suggesting the possible aggregation with process of aging or disease.

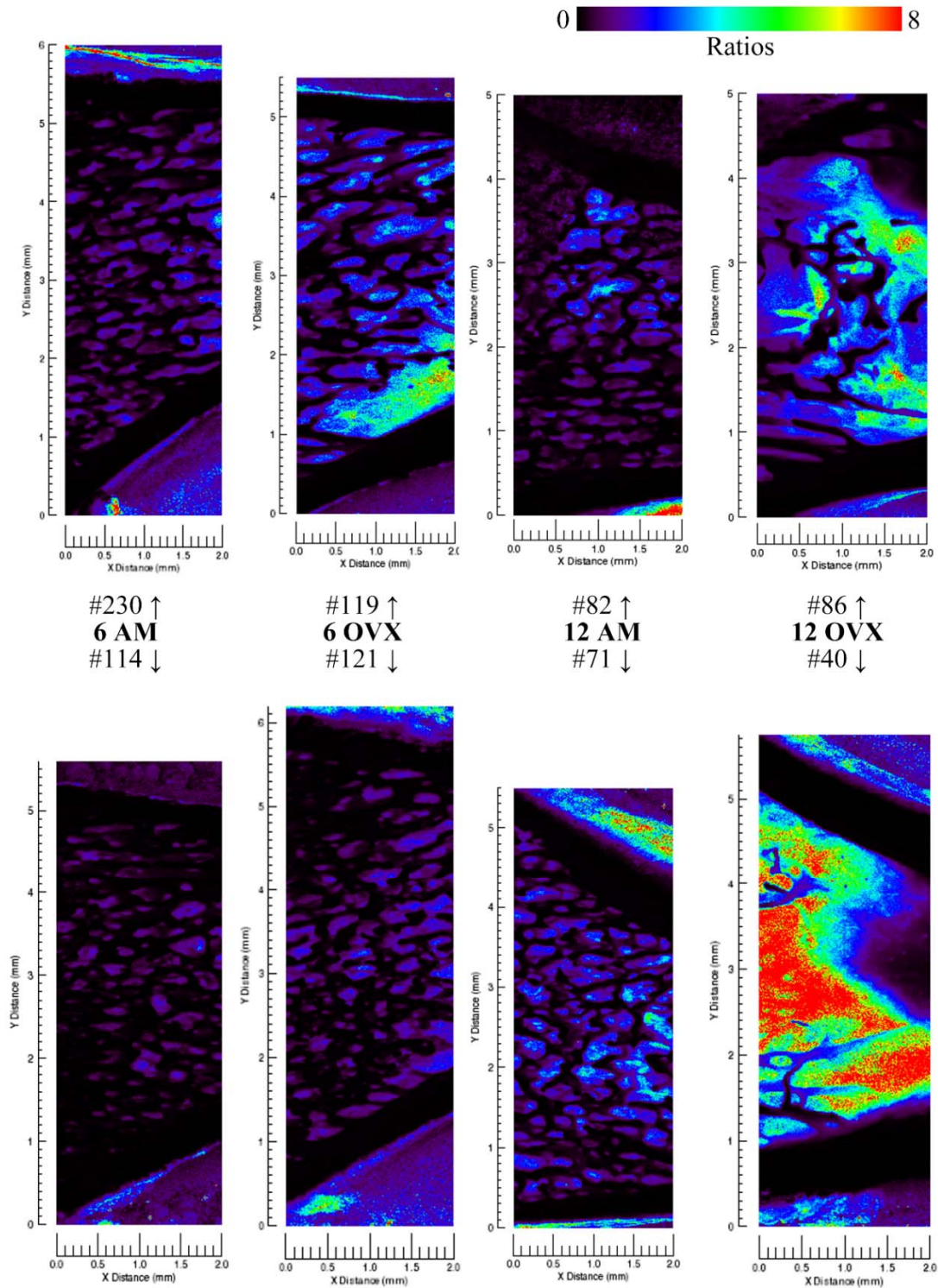


Figure 17 Zn/Ca ratio maps in color scale

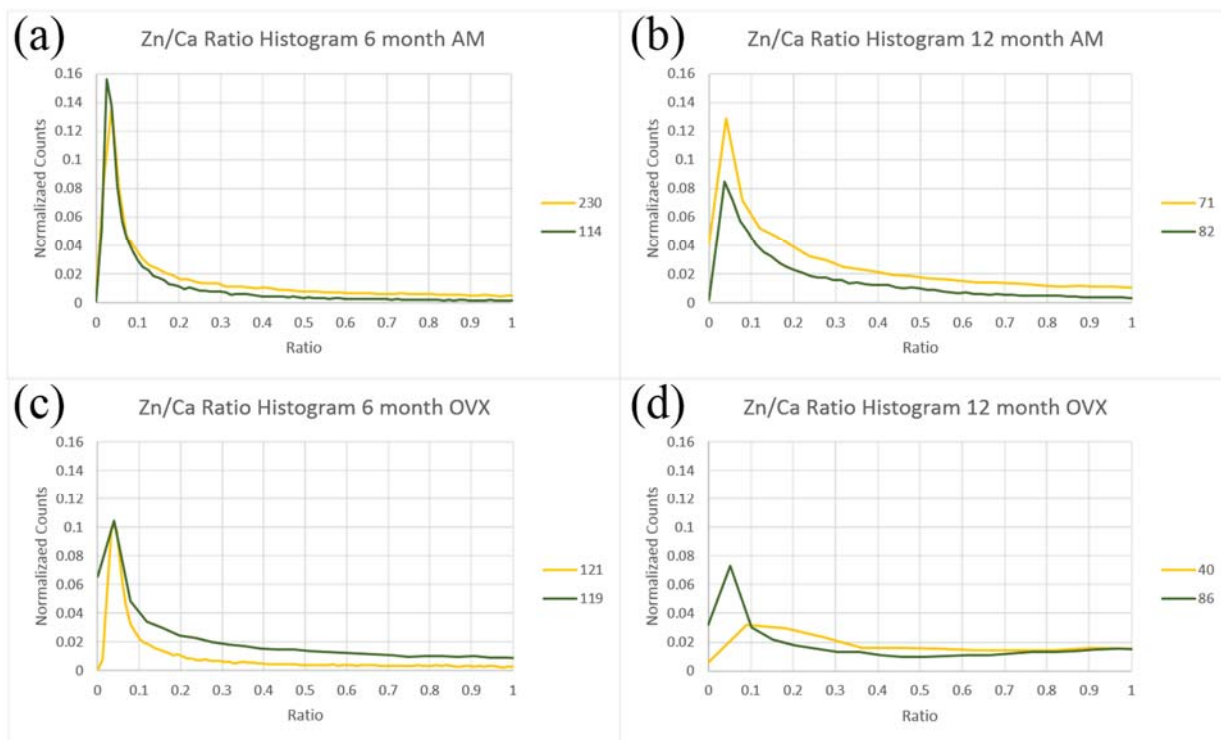


Figure 18 Curve for distribution of Zn/Ca ratio in different groups (a) 6 AM; (b) 12 AM; (c) 6 OVX; (d) 12 OVX

4.3.4 Quantification of elements

X-ray fluorescence method is capable of quantitative analysis besides qualitative analysis. The quantitative data is within reasonable ranges comparing with other research^{24,21}. Figure 19a shows spectra of 12 AM and 12 OVX groups. Comparing with healthy animals (red lines), ovariectomized rats (green lines) have lower intensities in Zn and higher intensities in Fe. Counts can be directly correlated to absolute amount of elements. Ca peaks are not shown in the diagram.

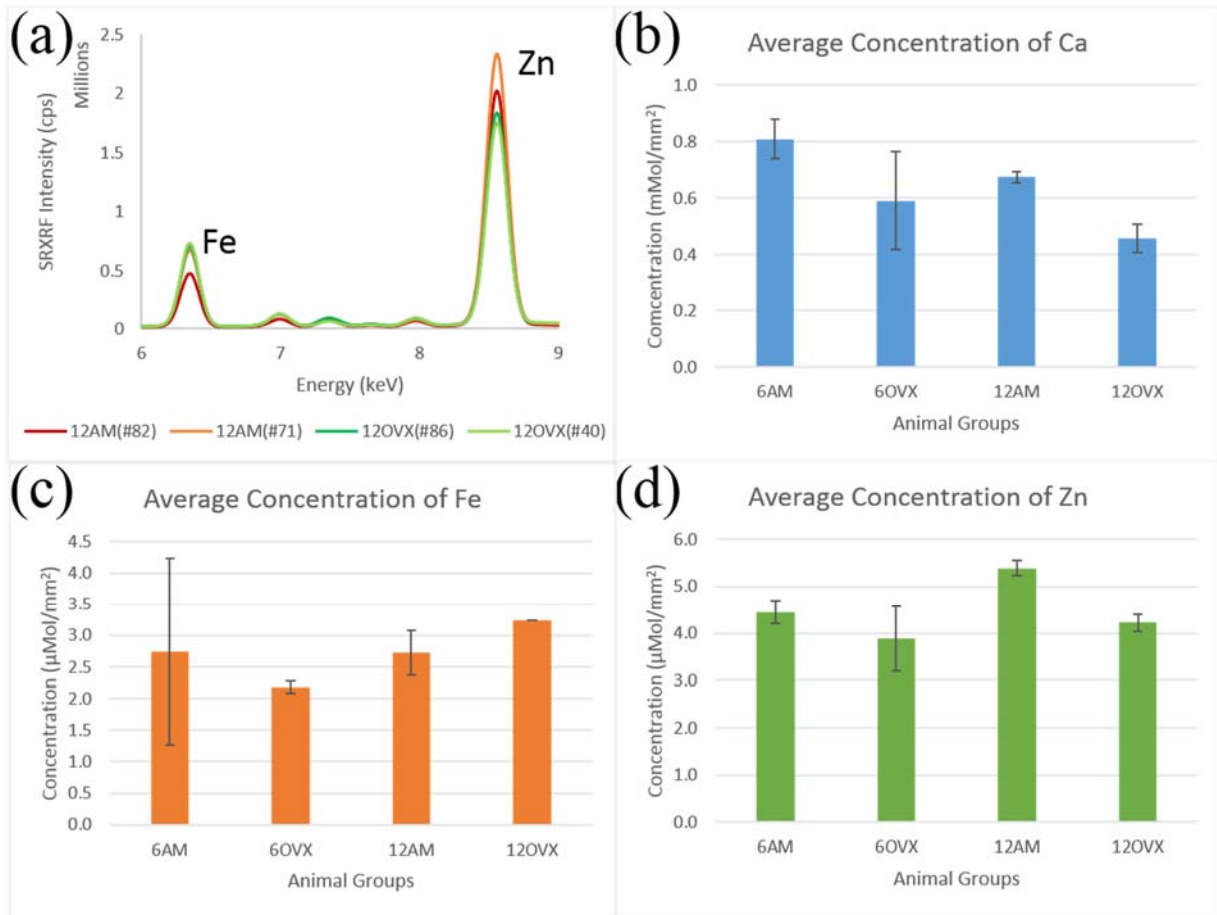


Figure 19 (a) SRXRF spectra of 12-month-age samples; and bar charts of average atomic molar concentration with standard deviation (error bar) of different elements (b) Ca; (c) Fe; (d) Zn ($n=2$)

Figure 19b shows the average atomic concentration of Ca. The error bar corresponds to the standard deviation of this mean values. It can be noticed that the amount of Ca declines with aging in both healthy and ovariectomized groups, yet cannot be recognized as significant ($p>0.1$). Changes in different health conditions at the same age can be observed. 6 OVX group is not statistically different with 6 AM group ($p>0.1$), probably because only 1 month after ovariectomizing isn't long enough to observe any symptoms obviously. However, it should be pointed out that decrease of Ca concentration from 12 AM to 12 OVX group can be regarded as a significant change ($p<0.05$). It is quite self-explanatory to understand that this trend is caused by bone mineral loss with aging process and osteoporosis.

Figure 19c shows the average atomic concentration of Fe. The error bar corresponds to the standard deviation of this mean values. It seems that Fe build up is not obvious with aging process in healthy groups ($p>0.1$), and is also not significant in 12 AM and 12 OVX groups ($p>0.1$). However OVX groups appear significant increase in Fe concentration when animals grow older ($p<0.05$). This may suggest Fe build up is more preferable to happen in osteoporotic bones.

Figure 19d shows the average atomic concentration of Zn. The error bar corresponds to the standard deviation of this mean values. Zn amount is generally increase with aging ($p<0.05$). Osteoporosis will result in decline in Zn amount, especially significant in 12-month-age animals ($p<0.05$). This trend agrees with other literatures indicating relations between osteoporosis and Zn amount.

CHAPTER 5 DISCUSSION

5.1 Fe and osteoporosis

Excessive Fe is thought to be toxic to bone as osteoporosis is a common complication in diseases caused by Fe overload. Abnormally high Fe may play a key role in postmenopausal osteoporosis in addition to estrogen deficiency⁴². Fe overload in bone is also known to people as ferric ion could facilitate osteoclast differentiation, inhibit osteoblast and alkaline phosphatase activities, and interfere with hydroxyapatite crystal growth and depositions³³. However, the Fe concentrations and distributions in osteoporotic bones are seldom studied.

In this thesis, an increase in Fe concentrations in OVX groups is observed. This agrees with many of other predictions and studies, but a study done by *Noor, et al.*²⁴. The differences may lie on different experiment methods, and since the decline trend they observed is not statistically significant ($p>0.5$) it may be caused by variations between patients.

It is known that Fe would build up with aging⁴³. A slightly but not obvious increase has been observed in AM groups, thus the significant increase in Fe amount in OVX groups cannot be raised only due to the accumulation over age. This indicates that a relationship between osteoporosis and Fe increase. Fe can interfere with bone metabolism in different manners, here is another hypothesis based on new findings in bone structure. *Davies, et al.*⁴⁴ reported a new findings that citrate anions together with water to create a viscous fluid in between nano-scale mineral platelets (see *Figure 20*). This viscous fluid might serve functions of slipping and shock absorbing, which is crucial in bone flexibility and maintenance under pressure. As citrate is known to retard the growth of hydroxyapatite⁴⁵, this citrate/water layer is also able to prevent minerals from getting too big to be brittle or broken. Based on this model, it is quite straight forward that Fe overload may easily leak out citrate, for the strong ability of citrate anions to chelate iron cations. Absence of citrate would result in increasing brittleness and risk of shattering, and might be a root cause of osteoporosis. To confirm this hypothesis, more study focusing on concentration on citrate anions should be done in the future.

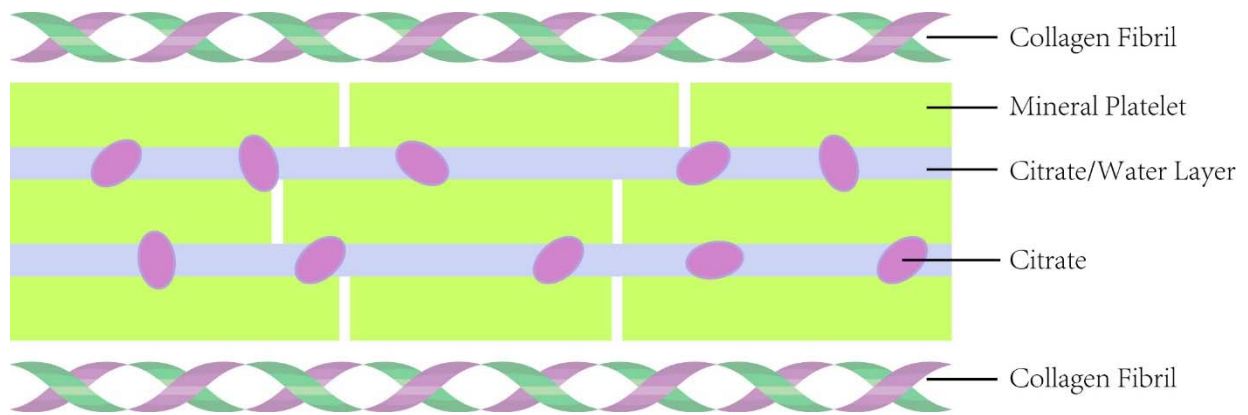


Figure 20 Briefly schematic diagram of new hypothesis of bone mineral (Illustrated by author based on the information and images from the reference⁴⁴)

On the other hand, Fe tends to accumulate in large pores in the bone. Although the mechanism of Fe increase in osteoporosis is still unknown, it can be assumed that this change in distribution could possibly result from absence of some inhibiting chemicals related to osteoporosis. According to the new bone structure model above, this inhibitor could be citrate anions in bone minerals. Hormones change would trigger Fe increase rapidly to break the chemical balance between citrate anions and iron cations, thus accelerate the loss of citrate over time. More study should be done to better understand the pathology of postmenopausal osteoporosis and its relationship with Fe increase to support this assumption.

5.2 Zn and osteoporosis

Zn is widely known as playing a positive role in bone metabolism. Bones contain plenty of Zn in both minerals, proteins and bone cells. Zn together with Ca and P forms minerals in bones, in the meanwhile is involved in protein frameworks that serve as scaffold for minerals to deposit on⁴¹. Moreover, Zn promotes osteoblast cell proliferation and differentiation by activating aminoacyl-tRNA synthetase, while inhibiting osteoclast cell activities. Also Zn forms alkaline phosphatase that does help to maintain bone metabolism²¹⁻²². However, there are little literature about the Zn concentrations and distributions in osteoporotic bones.

In this thesis, we observe an increase in Zn concentration as a function of aging in healthy groups ($p < 0.05$). This build up in Zn may result from an increase in bone tissue when animals become mature. Osteoporosis leads to a significant decline in Zn concentration when comparing 12 AM group and 12 OVX group, which agrees with prediction of most literatures. Locations of Zn can be roughly divided into in cortical bone, in trabeculae, in bone matrix framework and in the remaining places. From *Figure 16* it can be observed that great loss in trabeculae in osteoporotic bone, that will together lead to decline of Zn contained in the trabeculae. It can be also noticed that the protein framework is also losing its structure in OVX bone. When carefully studied sample #40 (12 OVX), it can be observed that Zn appears more detailed structure than Ca, indicating a higher loss rate in trabeculae than in framework in osteoporotic bone. Supporting evidence can be found in *Figure 21*. As Ca is known to decline with aging and osteoporosis, the increase in Zn/Ca ratio between AM groups and OVX groups indicates different loss rate in Zn. Decomposition of trabeculae is the main reason of losing minerals in osteoporosis, while the amount of Zn contained in trabeculae is less than in the protein matrix. As Zn and Ca contents in cortical bone can be regarded as constancy in all groups, it can lead to a hypothesis that osteoporotic bone will lose its minerals in trabeculae first, and then gradually lose its structural frame.

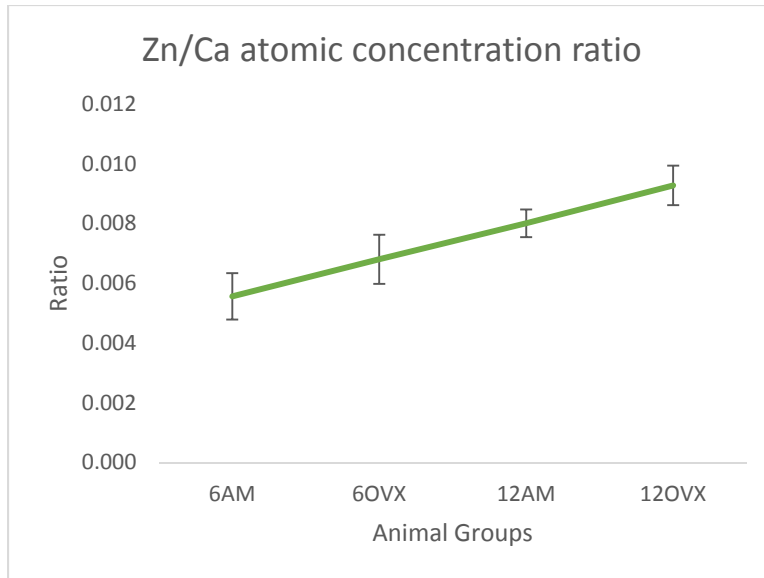


Figure 21 Zn/Ca atomic concentration ratio with standard deviation (error bar)

Zn distribution is also studied, and it can be seen that Zn tends to aggregate in area of endosteum (see *Figure 16*). Decomposition of trabeculae would release excessive Zn contained in bone minerals, and this observation may be due to the process of Zn excretory process. Excessive Zn will be transported through blood vessels located in cortical bone. Supporting evidence can be found in a study in women suffered osteoporosis⁴⁶. Urinary Zn excretion in osteoporosis group is 140 % higher than matched healthy group. That might hence explain the Zn distribution changes in osteoporosis.

CHAPTER 6 CONCLUSION AND FUTURE WORK

In this thesis, ovariectomized rat femur bones are used as a model of postmenopausal osteoporosis samples. SRXRF is used as a main technique to study the differences in concentrations and distributions in healthy and osteoporotic bones. After comparing Ca maps obtained from SRXRF with SEM, EDX and porosity calculated by Micro-CT, it can be concluded that SRXRF is a reliable method to study bone elements.

Typical changes from healthy to osteoporotic trabecular bone has been observed in Ca maps, and the decline in Ca concentration with aging and disease is quite self-explanatory. Fe accumulation over time is not significant in our observation, while Fe increase caused by OVX is quite obvious ($p < 0.05$). Aggregation of Fe in large pores caused by osteoporosis can be seen as well. Hypothesis based on a new finding about bone structure has been made. Citrate anions within bone minerals, which acting as inhibitor of exaggeration of mineral crystals, can chelate iron cations to raise brittleness of bones. Zn is built up with aging, and decreases in osteoporotic bone as predicted. It is also observed that Zn declines in a lower rate than Ca, and hypothesis has been made that osteoporotic bone will lose its minerals in trabeculae first, and then gradually lose its supporting protein structural frameworks. The trend that in OVX bones Zn migrates and aggregates around endosteum is seen as well, that may due to the excretory process of excessive Zn through blood vessels.

In the future, more animals from each group may be tested to ensure the findings above. Method of normalizing different samples can be optimized as well. To assist hypothesis on Fe increase with osteoporosis, the concentration changes in citrate anions should be studied. Process of Zn lose can be further understood by analyzing changes in Zn concentration of different bone tissues.

REFERENCES

1. Guyton, A. C., Textbook of medical physiology. *The American Journal of the Medical Sciences* **1961**, *242* (2), 136.
2. Angelo, G. Micronutrient and Bone Health. <http://lpi.oregonstate.edu/infocenter/bonehealth.html#>.
3. Wikipedia, Bone.
4. Heaney, R. P., Calcium, dairy products and osteoporosis. *Journal of the American College of Nutrition* **2000**, *19* (2 Suppl), 83s-99s.
5. Han, Z. H.; Palnitkar, S.; Rao, D. S.; Nelson, D.; Parfitt, A. M., Effects of Ethnicity and Age or Menopause on the Remodeling and Turnover of Iliac Bone: Implications for Mechanisms of Bone Loss. *Journal of Bone and Mineral Research* **1997**, *12* (4), 498-508.
6. Lieberman, S.; Bruning, N.; Bruning, N. P., *The Real Vitamin and Mineral Book: A Definitive Guide to Designing Your Personal Supplement Program*. Penguin: 2007.
7. UNICEF The State of the World's Children Fact Sheets. <http://www.unicef.org/sowc98/fs03.htm>.
8. Abraham, R.; Walton, J.; Russell, L.; Wolman, R.; Wardley-Smith, B.; Green, J. R.; Mitchell, A.; Reeve, J., Dietary determinants of post-menopausal bone loss at the lumbar spine: a possible beneficial effect of iron. *Osteoporosis International* **2006**, *17* (8), 1165-1173.
9. Nieves, J. W., Osteoporosis: the role of micronutrients. *The American journal of clinical nutrition* **2005**, *81* (5), 1232S-1239S.
10. New, S. A., Bone health: the role of micronutrients. *British medical bulletin* **1999**, *55* (3), 619-633.
11. Nieves, J., Nutrition and osteoporosis. *Osteoporosis: an evidence based approach to the prevention and management* **2002**.
12. Dawson-Hughes, B.; Dallal, G. E.; Krall, E. A.; Sadowski, L.; Sahyoun, N.; Tannenbaum, S., A controlled trial of the effect of calcium supplementation on bone density in postmenopausal women. *New England journal of medicine* **1990**, *323* (13), 878-883.
13. Nieves, J. W., Calcium and vitamin D: current developments in the prevention of osteoporosis and osteomalacia. *Current Opinion in Orthopaedics* **2004**, *15* (5), 383-388.
14. Palacios, C., The role of nutrients in bone health, from A to Z. *Critical reviews in food science and nutrition* **2006**, *46* (8), 621-628.
15. Fulgoni, V. L.; Keast, D. R.; Bailey, R. L.; Dwyer, J., Foods, fortificants, and supplements: where do Americans get their nutrients? *The Journal of nutrition* **2011**, *141* (10), 1847-1854.
16. Gür, A.; Çolpan, L.; Nas, K.; Çevik, R.; Saraç, J.; Erdoğan, F.; Düz, M. Z., The role of trace minerals in the pathogenesis of postmenopausal osteoporosis and a new effect of calcitonin. *Journal of bone and mineral metabolism* **2002**, *20* (1), 39-43.

17. Sandstead, H. H., Understanding zinc: recent observations and interpretations. *The Journal of laboratory and clinical medicine* **1994**, 124 (3), 322-7.
18. Prasad, A. S., Zinc: an overview. *Nutrition (Burbank, Los Angeles County, Calif.)* **1995**, 11 (1 Suppl), 93-9.
19. Maret, W.; Sandstead, H. H., Zinc requirements and the risks and benefits of zinc supplementation. *Journal of trace elements in medicine and biology : organ of the Society for Minerals and Trace Elements (GMS)* **2006**, 20 (1), 3-18.
20. Prasad, A. S.; Beck, F. W.; Grabowski, S. M.; Kaplan, J.; Mathog, R. H., Zinc deficiency: changes in cytokine production and T-cell subpopulations in patients with head and neck cancer and in noncancer subjects. *Proceedings of the Association of American Physicians* **1997**, 109 (1), 68-77.
21. Lowe, N. M.; Fraser, W. D.; Jackson, M. J., Is there a potential therapeutic value of copper and zinc for osteoporosis? *Proceedings of the Nutrition Society* **2002**, 61 (02), 181-185.
22. Li, X.; Sogo, Y.; Ito, A.; Mutsuzaki, H.; Ochiai, N.; Kobayashi, T.; Nakamura, S.; Yamashita, K.; LeGeros, R. Z., The optimum zinc content in set calcium phosphate cement for promoting bone formation in vivo. *Materials Science & Engineering C-Biomimetic and Supramolecular Systems* **2009**, 29 (3), 969-975.
23. Huckleberry, Y.; Rollins, C., Prevention of nutritional deficiencies. *Berardi, RR, DeSimone EM, Newton GD, et al. Handbook of Nonprescription Drugs* **2002**, 13, 483-484.
24. Noor, Z.; Sumitro, S. B.; Hidayat, M.; Rahim, A. H.; Sabarudin, A.; Umemura, T., Atomic Mineral Characteristics of Indonesian Osteoporosis by High-Resolution Inductively Coupled Plasma Mass Spectrometry. *Scientific World Journal* **2012**.
25. Shils, M. E.; Shike, M., *Modern nutrition in health and disease*. Lippincott Williams & Wilkins: 2006.
26. Coates, P. M., *Encyclopedia of dietary supplements*. CRC Press: 2005.
27. Benoist, B. d.; McLean, E.; Egl, I.; Cogswell, M., *Worldwide prevalence of anaemia 1993-2005: WHO global database on anaemia*. World Health Organization: 2008.
28. Crisponi, G.; Dean, A.; Di Marco, V.; Lachowicz, J. I.; Nurchi, V. M.; Remelli, M.; Tapparo, A., Different approaches to the study of chelating agents for iron and aluminium overload pathologies. *Analytical and Bioanalytical Chemistry* **2013**, 405 (2-3), 585-601.
29. Micronutrients, I. o. M. P. o.; Food, I. o. M.; Board, N., *DRI, Dietary Reference Intakes for Vitamin A, Vitamin K, Arsenic, Boron, Chromium, Copper, Iodine, Iron, Manganese, Molybdenum, Nickel, Silicon, Vanadium, and Zinc: A Report of the Panel on Micronutrients...[et Al.]*, Food and Nutrition Board, Institute of Medicine. National Academies Press: 2001.
30. Bacon, B. R.; Adams, P. C.; Kowdley, K. V.; Powell, L. W.; Tavill, A. S., Diagnosis and management of hemochromatosis: 2011 practice guideline by the American Association for the Study of Liver Diseases. *Hepatology (Baltimore, Md.)* **2011**, 54 (1), 328-43.

31. Tsay, J.; Yang, Z.; Ross, F. P.; Cunningham-Rundles, S.; Lin, H.; Coleman, R.; Mayer-Kuckuk, P.; Doty, S. B.; Grady, R. W.; Giardina, P. J., Bone loss caused by iron overload in a murine model: importance of oxidative stress. *Blood* **2010**, *116* (14), 2582-2589.
32. Kim, B. J.; Lee, S. H.; Koh, J. M.; Kim, G. S., The association between higher serum ferritin level and lower bone mineral density is prominent in women ≥ 45 years of age (KNHANES 2008 - 2010). *Osteoporosis International* **2013**, *24* (10), 2627-2637.
33. He, Y. F.; Ma, Y.; Gao, C.; Zhao, G. Y.; Zhang, L. L.; Li, G. F.; Pan, Y. Z.; Li, K.; Xu, Y. J., Iron Overload Inhibits Osteoblast Biological Activity Through Oxidative Stress. *Biological Trace Element Research* **2013**, *152* (2), 292-296.
34. Parelman, M.; Stoecker, B.; Baker, A.; Medeiros, D., Iron restriction negatively affects bone in female rats and mineralization of hFOB osteoblast cells. *Experimental Biology and Medicine* **2006**, *231* (4), 378-386.
35. Kharode, Y.; Sharp, M.; Bodine, P. N., Utility of the Ovariectomized Rat as a Model for Human Osteoporosis in Drug Discovery. In *Osteoporosis*, Westendorf, J., Ed. Humana Press: 2008; Vol. 455, pp 111-124.
36. Kwaczala, A. T. Alendronate and PTH Differentially Modulate Bone Quality and Reduce Adiposity in an OVX Rat Model. Ph.D., State University of New York at Stony Brook, Ann Arbor, 2012.
37. Chava, K. Material characterization of healthy and osteoporotic rat femur bone. M.S., State University of New York at Stony Brook, Ann Arbor, 2013.
38. NSLS Beamline X26A NSLS Configuration. <http://www.bnl.gov/x26a/config.shtml>.
39. Abraham, J.; Grenon, M.; Sanchez, H. J.; Perez, C.; Barrea, R., A case study of elemental and structural composition of dental calculus during several stages of maturation using SRXRF. *Journal of biomedical materials research. Part A* **2005**, *75* (3), 623-8.
40. Tommasini, S. M.; Trinward, A.; Acerbo, A. S.; De Carlo, F.; Miller, L. M.; Judex, S., Changes in intracortical microporosities induced by pharmaceutical treatment of osteoporosis as detected by high resolution micro-CT. *Bone* **2012**, *50* (3), 596-604.
41. Young, M., Bone matrix proteins: their function, regulation, and relationship to osteoporosis. *Osteoporosis International* **2003**, *14* (3), 35-42.
42. Jian, J. L.; Pelle, E.; Huang, X., Iron and Menopause: Does Increased Iron Affect the Health of Postmenopausal Women? *Antioxidants & Redox Signaling* **2009**, *11* (12), 2939-2943.
43. Liu, G.; Men, P.; Kenner, G. H.; Miller, S. C., Age-associated iron accumulation in bone: Implications for postmenopausal osteoporosis and a new target for prevention and treatment by chelation. *Biometals* **2006**, *19* (3), 245-251.
44. Davies, E.; Müller, K. H.; Wong, W. C.; Pickard, C. J.; Reid, D. G.; Skepper, J. N.; Duer, M. J., Citrate bridges between mineral platelets in bone. *Proceedings of the National Academy of Sciences* **2014**.

45. Tenhuisen, K. S.; Brown, P. W., The effects of citric and acetic acids on the formation of calcium-deficient hydroxyapatite at 38 °C. *J Mater Sci: Mater Med* **1994**, 5 (5), 291-298.
46. Szathmari, M.; Steczek, K.; Szücs, J.; Hollo, I., [Zinc excretion in osteoporotic women]. *Orvosi hetilap* **1993**, 134 (17), 911-914.